

# 小尺度公园对于城市热岛效应的缓解作用

## ——基于南京市中心城区社区公园的实证研究

# MITIGATION OF URBAN HEAT ISLAND EFFECT WITH SMALL-SCALE PARKS

## —AN EMPIRICAL STUDY ON COMMUNITY PARKS IN NANJING, JIANGSU PROVINCE

### 肖逸

南京林业大学风景园林学院风景园林学博士研究生

### 戴斯竹

南京林业大学风景园林学院风景园林学硕士研究生

### 赵兵\*

南京林业大学风景园林学院教授、博士生导师

### XIAO Yi

PhD Student in Landscape Architecture, College of Landscape Architecture of Nanjing Forestry University

### DAI Sizhu

Master Student in Landscape Architecture, College of Landscape Architecture of Nanjing Forestry University

### ZHAO Bing

Professor and PhD Supervisor, College of Landscape Architecture of Nanjing Forestry University

### \*通讯作者

地址：南京市玄武区龙蟠路159号南京林业大学风景园林学院

邮编：210037

邮箱：zhbn10118@njfu.edu.cn

### 摘要

城市化快速发展加剧了城市热岛效应，而城市绿地能够发挥重要的微气候调节功能。为探究小尺度公园的面积与形状对热岛效应的缓解作用，本文以江苏省南京市中心城区的社区公园为例，选取2019年Landsat 8-OLI遥感影像数据进行地表温度反演，借助ArcGIS 10.4识别52个社区公园，并以核建筑密度估计法对社区公园进行分类，探讨缓解城市热岛效应的最佳社区公园面积阈值和形状规律。结果表明：1) 随着社区公园缓冲带距离的增加，降温强度逐渐减弱，降温范围多在0~180m；2) 面积、形状、归一化植被指数是影响公园降温强度的重要因素；3) 高核建筑密度的社区公园降温强度更佳，且面积阈值（0.848hm<sup>2</sup>）大于低核建筑密度的社区公园（0.384hm<sup>2</sup>）；4) 社区公园形状趋于圆形或正方形时，降温效果显著。因此，在城市绿地系统规划层面，建议在高建筑密度区域合理规划小尺度的公园绿地，精细化的存量设计与管理有助于发挥城市区域的最佳生态效益，能更好地缓解局部热岛效应。

### 关键词

社区公园；基于自然的解决方案；城市热岛效应；微气候调节；实证研究

### ABSTRACT

Cities have suffered from urban heat island (UHI) effect due to rapid urbanization, which can be effectively adjusted by urban green space. Taking the community parks in central area of Nanjing, Jiangsu Province as an example, this paper explored the size and shape of small-scale parks to mitigate the UHI effect. Land surface temperature was retrieved from Landsat 8-OLI remote-sensing image of 2019. The 52 studied community parks were identified with ArcGIS 10.4, and classified by kernel building density. The threshold-size and optimal shape of community parks to mitigate UHI effect were then discussed. The results showed that 1) with the increase of buffer ring distance around the community parks, the cooling intensity decreased and the cooling extent were mostly less than 180 m; 2) the area, shape, and the NDVI of the parks were important factors affecting the cooling intensity; 3) the cooling intensity of community parks under a high kernel building density was better, with a higher threshold-size (0.848 hm<sup>2</sup>) than that of the low ones (0.384 hm<sup>2</sup>); and 4) the optimal cooling intensity would occur when the park in a shape of circle or square. In conclusion, it is suggested that small green space should be planned in the areas under a high building density. Through renewal design and refined management measures in the urban green space system planning, giving full play to the ecological benefits of urban green spaces in mitigating the local UHI effect can also be expected.

### KEYWORDS

Community Park; Nature-Based Solutions; Urban Heat Island Effect; Microclimate Adjustment; Empirical Study

### 基金项目

中华人民共和国国家林业局软课题“生态文明与美丽城乡建设创新管理体制研究”（编号：2016-R32）  
江苏高校优势学科建设工程资助项目

### RESEARCH FUNDS

Research on the Innovation Management System of Ecological Civilization and Beautiful Urban and Rural Construction, Soft Scientific Topics of the State Forestry Administration of the People's Republic of China (No. 2016-R32)  
A Project Funded by the Priority Academic Program Development (PAPD) of Jiangsu Higher Education Institutions

编辑 冉玲于 翻译 田乐 冉玲于 肖逸

EDITED BY RAN Lingyu TRANSLATED BY Tina TIAN RAN Lingyu XIAO Yi

## 1 引言

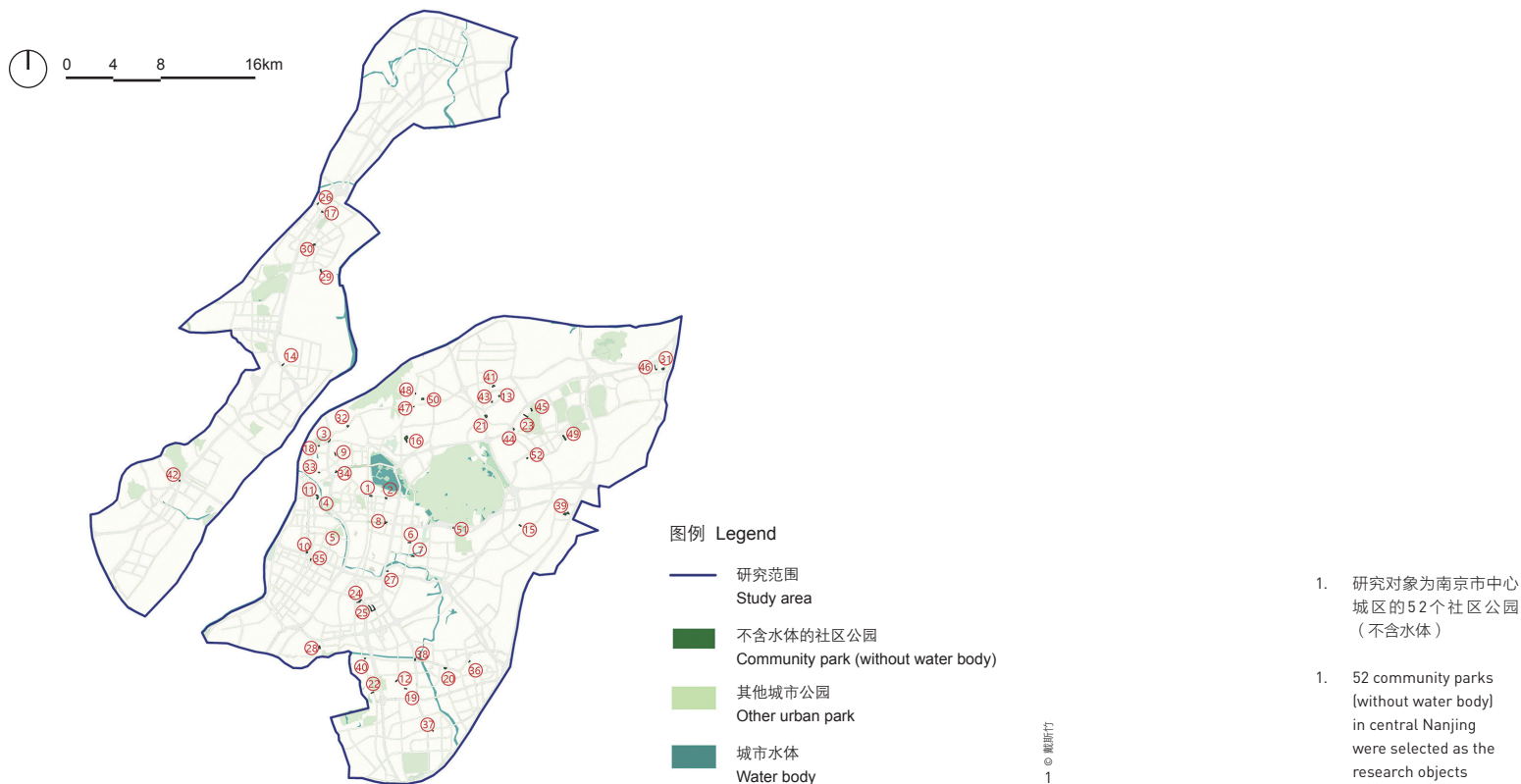
2018年修订的《世界城市化展望》报告中提出全球城市化正迅速发展,世界城市人口在世界总人口中占比高达55%,预计至2050年将达到68%,届时,中国城镇人口总量将高达10.86亿<sup>[1]</sup>。快速城市化影响了景观格局的演变,城市绿地不断缩减,城市生态系统平衡遭到破坏,热岛效应等生态问题也日渐突出<sup>[2]</sup>。抵御自然灾害的传统工程化手段不仅成本巨大,而且效果欠佳<sup>[3]</sup>。近年来,“基于自然的解决方案”(NBS)受到越来越多的学者和城市规划决策者的重视,通过发挥生态系统自身的服务功能,使经济、环境和社会实现可持续发展<sup>[4][5]</sup>,这种生态措施也更符合成本效益原则<sup>[6]</sup>。

目前,大量研究证实了城市绿地能有效调节城市微气候(如缓解城市热岛效应)<sup>[7]</sup>,其在协助城市应对未来气候变化的过程中扮演着极为重要的角色<sup>[8]</sup>。如张昌顺等人以北京为例,分别将中心城区、卫星城及郊区作为研究对象,试图揭示城市绿地降温幅度与绿地类型(包括草地、乔木林、乔草、乔灌、乔灌草、灌木林、竹丛)、绿地结构及管理措施的内在联系<sup>[9]</sup>;马吉德·阿玛尼—贝尼等人发现城市公园的降温效果与绿地类型(包括林地、草地、城市公园)和景观指数显著相关<sup>[10]</sup>;杜红玉以上海市地表温度的时空分布格局为基础,讨论基于景观格局指数的城市蓝绿空间冷岛效应,并提出了有效的规划对策<sup>[11]</sup>。同时,其他研究进一步发现城市绿地的面积、形状等是影响其降温效果的重要因素<sup>[12]-[14]</sup>。周东颖等人重点分析了城市公园对周围环境温度的调控效应,揭示了公园内部温度与面积的定量关系<sup>[15]</sup>;张志如等人认为城市绿地的降温效果与其面积之间可能呈非线性关系<sup>[16]</sup>。余兆武等人提出效率的阈值(TVoE)这一概念,即当城市绿地面积大于某一临界值时,其单位面积的降温强度将显著下降。这一结论加强了城市生态研究和规划设计实践之间的联系<sup>[17]-[19]</sup>,使城市规划和城市绿地系统规划更加注重公园本身面积和形状等因素对热岛效应的缓解作用。

## 1 Introduction

In 2018, 55% of the world population reside in cities, and the predicted number will reach 68% by 2050 as the urban population of China will reach 1.086 billion, reported in the World Urbanization Prospects 2018<sup>[1]</sup>. Rapid urbanization has impacted the evolution of cities' landscape pattern, sharply shrinking urban green spaces and accompanying severe ecological problems such as the exacerbated urban ecosystem damage and urban heat island (UHI) effect<sup>[2]</sup>. Moreover, traditional costly approaches that aim to resist natural disasters are no longer effective in coping with today's environmental challenges<sup>[3]</sup>. In response, "Nature-Based Solutions" (NBS) has attracted increasing attention of researchers and planning decision-makers over recent years. Leveraging and facilitating the delivery of ecosystem services, NBS can contribute to the sustainability of economy, environment, and society<sup>[4][5]</sup>, and is widely regarded as ecological measure of a sound cost-effectiveness<sup>[6]</sup>.

A large number of studies have proven that urban green space can effectively regulate urban microclimate (e.g., UHI effect mitigation)<sup>[7]</sup>, being a critical component to a city's resilience to future climate changes<sup>[8]</sup>. For example, Zhang Changshun et al. examined the central area, satellite towns, and suburbs of Beijing City and attempted to reveal the inner-relations between the cooling intensity of green space with its type (include grass, arbor forest, arbor-grass, arbor-shrub, arbor-shrub-grass, shrub, and bamboo forest), structure, and management measures<sup>[9]</sup>; Majid Amani-Beni et al. found that the cooling effect of urban parks has a significant correlation with the urban green space type (farmland, waterbody, and urban green space) and its landscape level index<sup>[10]</sup>; Du Hongyu probed into the cool island effect of green-blue spaces and their optimal distributions based on landscape pattern index, i.e. spatial and temporal pattern of land surface temperature, and proposed associated planning strategies<sup>[11]</sup>. Studies have also proven that the size and shape of urban green space are key factors to its cooling effect<sup>[12]-[14]</sup>. Zhou Dongying et al. quantified the correlations between the size and temperature of urban parks in cooling effect<sup>[15]</sup>; Furthermore, Chang Chi-Ru et al. found that there may be a non-linear relation in urban green space area and the cooling effect<sup>[16]</sup>; Yu Zhaowu et al. defined a threshold value of efficiency (TVoE), i.e. the cooling efficiency will decrease when the size of urban green space exceeds a critical value—This finding bridges urban ecological research and landscape planning and design practice<sup>[17]-[19]</sup>, and the mitigation on UHI effect by parks is broadly explored (especially in size and shape) in urban land planning and urban green space system planning.



总体来看, 已有研究多集中于现有景观组成和空间配置对案例城市热岛效应的缓解作用, 亦有少数学者开始着眼于量化水体、绿地等不同景观类型的面积阈值, 以便获得绿地最佳降温效果, 有利于进一步的城市管理和气候适应性规划的制定<sup>[20]-[22]</sup>。但是, 针对小尺度的绿地面积和形态与降温效果之间的量化研究尚且不足。因此, 本文以南京市中心城区社区公园为例, 旨在1) 探究社区公园对周边环境降温效果的影响因素; 2) 量化、讨论社区公园的最佳面积、形状; 3) 为绿地规划在城市微气候调节功能上提出可行建议, 帮助更有效地缓解城市热岛效应, 并提供数据支撑与方向指引。

## 2 研究区域与研究方法

### 2.1 研究区域

南京市地处长江下游, 属于典型亚热带季风性气候, 年平均气温15.4℃。随着近年多个城市中心的快速发展, 城市热岛效应加剧, 素有“火炉”之称的南京已成为中国夏季最炎热的城市之一。2019年

In general, current literature mainly studies the composition and configuration of existing urban landscapes to the mitigation on UHI effect. Also, a few of studies quantify the threshold-size in different landscape types (e.g., waterbody and green space) to the optimal cooling effect of green space to better supply urban management and climate adaptation planning<sup>[20]-[22]</sup>. However, there are few documents on quantizing the relation between the cooling effect with the area and shape of small-scale green spaces. The authors selected the existing community parks in the central area of Nanjing as an example to 1) identify the causal factors of community parks on the urban cool island (UCI) effect to surrounding environment; 2) quantify the threshold-size and optimal-shape of community parks; and 3) offer references to urban green space planning on mitigating UHI effect and improving microclimates with quantitative evidences and guidance on adaptive strategies.

## 2 Study Area and Research Methods

### 2.1 Study Area

Located in the lower reach of the Yangtze River, Nanjing has a typical subtropical monsoon climate and its annual average temperature is 15.4℃. In recent years, with the rapid expansion of several urban centers that have aggravated the UHI effect,

- ① 南京市公安局统计数据：2019年底，南京市实有人口1031.22万人，常住人口850.00万人，流动人口321.40万人。
- ② 依据《城市绿地分类标准CJJT85-2017》选取。社区公园（G12）指用地独立，具有基本的游憩和服务设施，主要为一定社区范围内居民就近开展日常休闲活动服务的绿地，规模宜大于1hm<sup>2</sup>。
- ③ 数据来源：USGS官网
- ④ 研究采用了遥感影像图和高分辨率卫星影像，原因是Landsat 8-OLI的分辨率为30m（对于反演LST而言已足够），而BIGEMAP地图数据软件提取的影像图分辨率可达0.5m，适于提取面积较小的社区公园。

- ① Statistics of Nanjing Public Security Department: By the end of 2019, Nanjing had a population of 10,312 million, including a resident population of 8.5 million and a migrant population of 3.214 million.
- ② According to the Standard for Classification of Urban Green Space (CJJT85-2017), community park (G12) refers to the green space that is independently-planned in land use [better larger than 1 hm<sup>2</sup>] and has daily leisure and recreational facilities and supporting services, mostly used by the residents living in surrounding communities.
- ③ Source: the official website of United States Geological Survey (USGS)
- ④ Remote sensing image and high-resolution satellite image were both used in this research; the resolution of the remote-sensing image obtained from the Landsat 8-OLI is 30 m that is accurate enough for LST retrieval, and the resolution of satellite image extracted from the BIGEMAP is 0.5 m, which is more suitable for identifying small-scale community parks.

底，南京实有人口突破千万<sup>①</sup>，中心城区人口尤甚稠密。因此，为了探讨城市小尺度公园对热岛效应的影响，本文以居民日常生活中使用频率较高的社区公园作为研究对象。据统计，南京中心城区面积约834km<sup>2</sup>，包含609个公园，其中社区公园<sup>②</sup>共62个（单个公园面积集中在1.02hm<sup>2</sup>~9.66hm<sup>2</sup>之间），数量占比10.18%，而面积仅占中心城区公园总面积的1.81%。这些公园散布于城区各个角落，其降温效果将直接影响到周边居民对其的日常使用情况。此外，洛厄尔·W·亚当斯等人提出包含水体的绿地将加强降温效果<sup>[23]</sup>。因此，为消除此类绿地对研究结果的干扰，本文从南京市中心城区现有的62个社区公园中，选取了52个不含水体的社区公园作为最终测算对象（图1）。

## 2.2 数据来源与初步处理

本研究用于地表温度反演的遥感影像来自美国地质调查局<sup>③</sup>的Landsat 8-OLI，分辨率为30m，成像时间为2019年7月11日，天气晴热无云，最低温度23℃，最高温度30℃。初步利用ENVI 5.3对热红外波段以外的其他波段进行辐射定标和大气校正，并于ArcGIS 10.4中按掩膜提取出南京市中心城区。用于社区公园识别的2019年南京市中心城区高分辨率（分辨率为0.5m）卫星影像，则提取自BIGEMAP地图数据软件<sup>④</sup>，初步利用ArcGIS 10.4对该卫星影像进行坐标转换、地理配准等操作。

## 2.3 研究方法

本研究基于Landsat 8-OLI遥感影像和高分辨率卫星影像，利用ArcGIS 10.4和ENVI 5.3获取地表温度、社区公园位置、核建筑密度等数据，并采用SPSS 24.0和Excel进行统计分析，以找寻小尺度城市公园的冷岛效应与其面积、形状等特征之间的联系。

### 2.3.1 地表温度反演

鉴于Landsat 8-OLI中适合进行分裂窗口算法的第11波段的参数设置不稳定，而适宜在大气水蒸气含量较低情况下使用的单通道算法在南京市雨水丰沛的夏季也并不适用<sup>[24]</sup>，因此，为获取具有较高精确度的地表温度（LST）<sup>[25]-[27]</sup>，本研究采用辐射传输方程法（RTE）在ENVI 5.3中对第10波段进行地表温度反演<sup>[28]</sup>。

Nanjing is one of the hottest cities in China. By the end of 2019, the residing population of Nanjing exceeded 10 million<sup>①</sup>, and most of them lived in the central area of the city. To explore the mitigation of small-scale urban parks on the UHI effect, this paper studied on the community parks within the city which are the daily places for citizens' leisure life. The central Nanjing covers an area of about 834 km<sup>2</sup> and has 609 parks, 62 of which are community parks<sup>②</sup>—ranging from 1.02 hm<sup>2</sup> to 9.66 hm<sup>2</sup>, only accounting for 1.81% of the total park area in the study area. These community parks are scattered throughout the city center, and their cooling effect directly affects citizens' daily use of leisure and recreational places. Considering that the cooling effect of water bodies would confuse the research results, as the findings by Lowell W. Adams et al.<sup>[23]</sup>, this study further excluded 10 of the 62 community parks which cover water bodies (Fig. 1).

## 2.2 Data Sources and Pre-Processing

Remote-sensing images of central area of Nanjing used in this study include Landsat-8 OLI one (30 m in resolution) and high-resolution satellite one (0.5 m in resolution) obtained from the USGS Earth Explorer<sup>③</sup> and BIGEMAP data software<sup>④</sup>, respectively. The former one was taken on July 11th, 2019 when the weather was sunny and cloudless, and the detected temperature was 23 ~ 30℃; all bands except the thermal infrared one were processed in ENVI 5.3 for radiometric calibration and atmospheric correction, then obtained the image of central Nanjing by mask extraction with ArcGIS 10.4. The latter one was obtained through the coordinate transformation and geographical registration by ArcGIS 10.4.

## 2.3 Study Methods

Based on the remote-sensing image and the high-resolution satellite image, the study attained land surface temperature (LST), community park location, kernel building density, and other data with ArcGIS 10.4 and ENVI 5.3. The relations between the UCI of small-scale urban parks with their size and shape factors were explored through the statistical analysis with SPSS 24.0 and Excel.

### 2.3.1 Land Surface Temperature Retrieval

Due to the unstable parameter settings in band 11 of the Landsat 8-OLI satellite, and the single-channel algorithms suitable for the situation of low atmospheric water vapor content being not applicable for the rainy weather of Nanjing<sup>[24]</sup>, the study introduced the radiative transfer equation (RTE)<sup>[28]</sup> to retrieve a highly accurate land surface temperature (LST)<sup>[25]-[27]</sup> using band 10 in ENVI 5.3.

### 2.3.2 社区公园识别与缓冲区划定

通过2019年的南京市卫星影像、《南京市公园布局规划（2017-2035）》，以及现场调研，进一步精确获取社区公园信息，借助ArcGIS 10.4识别社区公园，并计算社区公园面积。此外，考虑到Landsat 8-OLI图像的最小分辨率为30m<sup>[14][18]</sup>，分别沿社区公园边界每隔30m向外生成缓冲带，得到总距离为600m的20个多环缓冲带，即设定0~600m为社区公园缓冲区<sup>⑤</sup>，以便提取各缓冲带的地表温度，计算每个社区公园的降温范围和强度。

### 2.3.3 核建筑密度估计

地表温度是区域土地利用和人为热的综合体现，因此，社区公园周围的建筑分布情况对于降温强度具有一定影响。本研究采用了黄焕春等人提出的“核建筑密度”的概念与算法<sup>[29]</sup>。其概念来源于“核密度估计法”<sup>⑥</sup>，指空间上某点的建筑密度是以该点为圆心的一定距离内，总建筑基底面积与该范围内用地面积的比值；算法采用核密度函数的计算思想，基于栅格数据格式，运用移动搜索法对面域单元空间进行逐个像元计算，具体而言是以某点（*i*点）为中心画一个圆形作为滤波

### 2.3.2 Community Parks Identification and Buffer Zone Parameter Delineation

According to the high-resolution satellite image, the schemes of Nanjing Park Layout Planning (2017-2035), and field surveys, the location and area of the 52 community parks were identified with the ArcGIS 10.4. Moreover, considering the 30 m as the minimum resolution of Landsat image<sup>[14][18]</sup>, 20 buffer rings (each with a width of 30 meters) were set for each community park, i.e. the width of the total buffer zone of each park ranged from 0 to 600 m<sup>⑤</sup>. The average LST in each buffer zone was retrieved to quantify the cooling extent and intensity.

### 2.3.3 Kernel Building Density Estimation

LST is subject both to local land use and anthropogenic heat. The cooling intensity of a community park is affected by the building environment around it. This study adopted the concept and algorithm of “kernel building density,” proposed by Huang Huanchun et al.<sup>[29]</sup> based on the theory of kernel density estimation<sup>⑥</sup>. The building density of a certain place is the ratio of the total building area to the land area within a certain distance centered from the place. Applying the kernel density function, the method of floating catchment area (FCA) is used to calculate the unit space of the area one by one on the raster data format. Specifically, a circle can be drawn centered on one point (*i*) as the

⑤ 基于反演得到的LST数据分辨率为30m，研究将缓冲带宽度设为30m；根据初步研究发现最大降温范围基本为300m以内，个别公园大于400m，出于研究结果准确性的考虑，最终将缓冲区最大范围设定为600m。

⑥ 核密度估计法可用于计算人口密度、建筑密度，获取犯罪情况报告，监测旅游区人口密度等。具体是通过计算点、线要素测量值在指定邻域范围内的单位密度，来直观反映离散测量值在连续区域内的分布情况（参见参考文献[29]）。

⑤ To improve the research accuracy, the width of a buffer ring was determined according to the resolution of the retrieved LST data (30 m). The data pre-processing found that the maximum cooling extent of the studied parks was mostly less than 300 meters but exceeding 400 meters for a few of samples; for a higher research accuracy, the study examined a 600-meter-width buffer zone for each park.

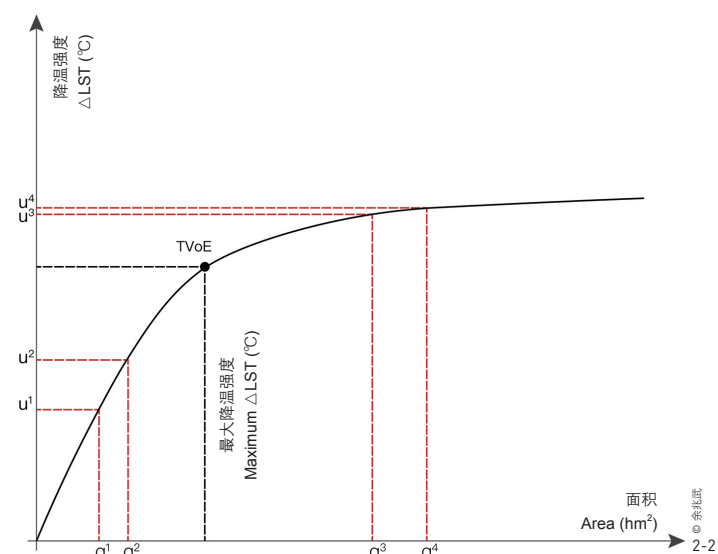
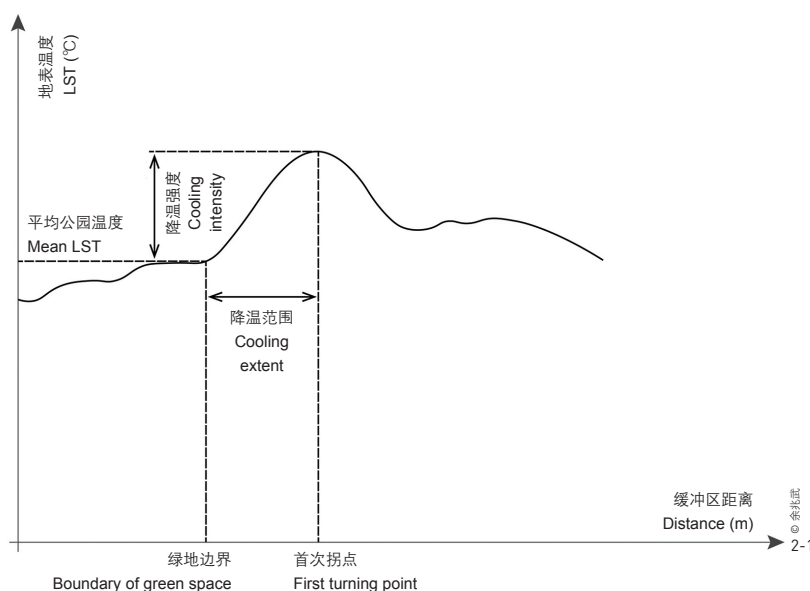
⑥ The kernel density estimation method can be used to estimate population and building density, predict crimes, and monitor visits in tourist areas. It can analyze point-based or line-based data in a neighborhood to map a continuous random variable [Source: Ref. [29]].

表1: 斑块尺度下景观格局特征指数及其生态学涵义  
Table 1: The characteristic indexes of landscape pattern and their ecological implication at the patch scale

指数名称 Name of index	定义 Definition	数值范围 Range
斑块面积 Patch area	度量单位: m <sup>2</sup> 或hm <sup>2</sup> Unit: m <sup>2</sup> / hm <sup>2</sup>	A ≥ 0
斑块紧凑度指数 Patch Compactness Index (CI)	$CI = \frac{2\sqrt{\pi A}}{P}$ 式中, A表示斑块面积, P表示斑块周长。CI越小表示斑块形状越不紧凑, 当斑块为圆形(即CI为1)时形状最紧凑 A is the patch area and P is the patch perimeter. The smaller the CI is, the less compact the patch shape is. It is the most compact when the patch is circular (i.e. CI is 1)	0 ≤ CI ≤ 1
景观形状指数 Landscape Shape Index (LSI)	$LSI = \frac{E}{2\sqrt{\pi A}}$ 式中, E为景观中所有斑块边界的总长度, A为景观总面积。LSI=1时为圆形; LSI=1.13时为正方形; LSI值越大, 形状越不规则 E is the total length of all patch boundaries in the landscape and A is the total landscape area. When LSI equals 1, it is a circle; when LSI equals 1.13, it is a square; the larger the LSI is, the more irregular the landscape shape is	LSI ≥ 1
地表温度 Land Surface Temperature (LST)	$LST = \frac{K_2}{\ln\left(\frac{K_1}{B(T_s + 1)}\right)}$ 对Landsat-8 OLI band 10来说, K <sub>1</sub> = 774.89(mW · m <sup>-2</sup> · sr <sup>-1</sup> · um <sup>-1</sup> ), K <sub>2</sub> = 1321.08K, 且T <sub>s</sub> 是地面辐射 For the Landsat-8 OLI band 10, K <sub>1</sub> = 774.89(mW · m <sup>-2</sup> · sr <sup>-1</sup> · um <sup>-1</sup> ), K <sub>2</sub> = 1321.08K, T <sub>s</sub> is the ground radiation	LST ≥ 0
归一化植被指数 Normalized Difference Vegetation Index (NDVI)	$NDVI = \frac{(\rho_{NIR} - \rho_{RED})}{(\rho_{NIR} + \rho_{RED})}$ 式中, NIR为近红外波段的反射值, RED为红光波段的反射值。当NDVI为负值时表示地面覆盖为云、水、雪等, 正值表示植被覆盖 NIR is the reflected value of near-infrared band, and RED is the reflected value of red light band. When the NDVI is a negative value, the ground cover is cloud, water, snow, etc., while the positive value is vegetation cover	-1 ≤ NDVI ≤ 1

2. 论文采用余兆武等人于2017年提出的城市冷岛效应范围、强度和效率的阈值 (TVoE) 的概念曲线研究降温强度。q<sup>1</sup>到q<sup>2</sup>面积增加伴随着较大的降温强度变化 (u<sup>2</sup>-u<sup>1</sup>), q<sup>2</sup>到q<sup>4</sup>面积增加伴随着较小的降温强度变化 (u<sup>4</sup>-u<sup>3</sup>), 且q<sup>2</sup>-q<sup>1</sup>的面积等于q<sup>4</sup>-q<sup>3</sup> (参见参考文献[17])。

2. The conceptual curve of urban cooling island extent, intensity, efficiency, and TVoE proposed by Yu Zhaowu et al. [2017] is adopted in this paper. The q<sup>1</sup> to q<sup>2</sup> equals q<sup>3</sup> to q<sup>4</sup>, u<sup>2</sup>-u<sup>1</sup> is greater than u<sup>4</sup>-u<sup>3</sup> [Source: Ref. [17]].



窗口 (A), 用窗口内的平均值作为该点的核建筑密度值 (x<sub>i</sub>), 最后可得到空间变化连续的核建筑密度变化图。其计算公式如下:

$$\hat{f}(x) = \frac{1}{nh^d} \frac{\sum_{i=1}^n K(w_i x_i)}{A}$$

式中, K()为核密度函数; w<sub>i</sub>为空间i的权重值, x<sub>i</sub>为i点的核建筑密度, A为滤波窗口的面积, h为空间作用的阈值范围, n为阈值范围内的点数, d为数据的维数。

此外, 为了研究不同核建筑密度下社区公园的最佳面积阈值与形状, 本研究提出对公园周边缓冲区 (0~600m) 内的核建筑密度在ArcGIS 10.4中按照自然间断点分级法进行量化, 分为低核建筑密度的社区公园 (核建筑密度为0~17 923, 共38个) 和高核建筑密度的社区公园 (核建筑密度为17 924~81 613, 共14个)。

### 2.3.4 降温强度量化及相关影响因素

城市热岛效应的缓解与绿地面积、形状等因素有关<sup>[30][31]</sup>, 但尚未明确绿地在何种条件下具有最大降温效果, 以及形状、面积如何影响降温强度<sup>[22][32]</sup>。本研究借助ArcGIS 10.4和FRAGSTATS计算反映斑块形

filtering window (A), using the average value in the window A as the kernel building density to point i. Finally, a kernel building density diagram with continuous spatial changes was obtained. The calculation formula is as follows:

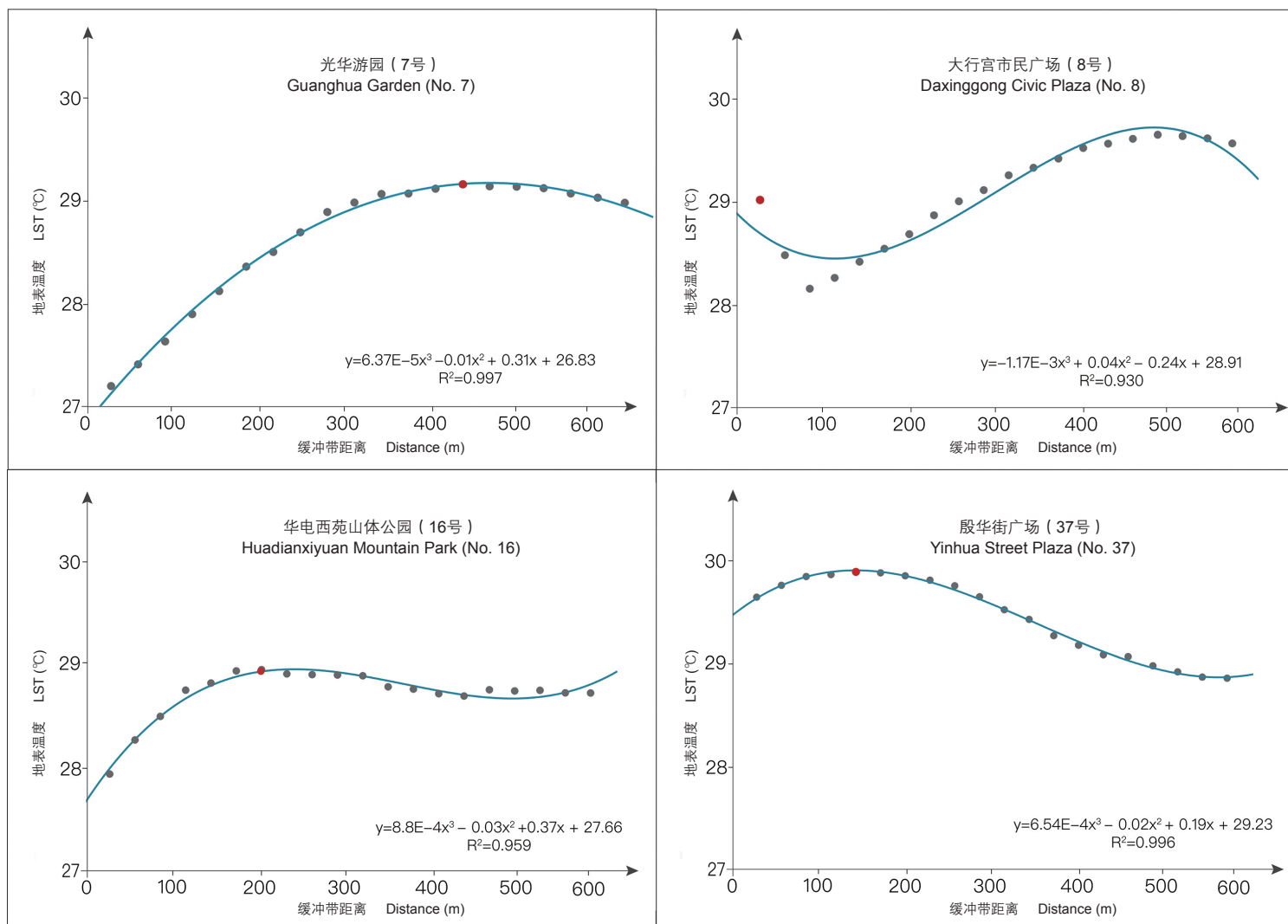
$$\hat{f}(x) = \frac{1}{nh^d} \frac{\sum_{i=1}^n K(w_i x_i)}{A}$$

where, K() is the kernel density equation; w<sub>i</sub> is the weight value of place i, x<sub>i</sub> is the kernel building density of point i, A is the size of filtering window, h is the threshold range of spatial effect, n is the number of points in the threshold range, and d is the dimension of data.

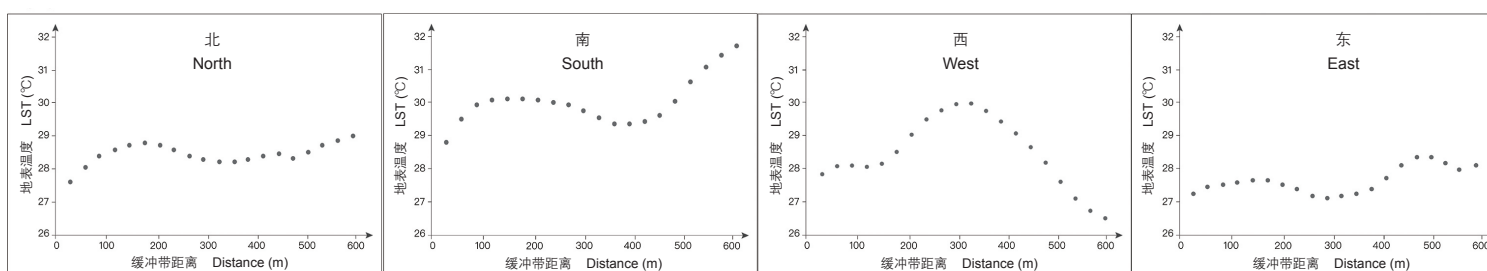
In addition, in order to identify the threshold-size and optimal shape of community parks under different kernel building densities, this study quantified the kernel building density within the buffer zone (0 ~ 600 m) around the community parks by the natural breaks in ArcGIS 10.4. Finally, 38 community parks were identified under a low kernel building density (kernel building density values 0 ~ 17,923) and 14 under a high kernel building density (kernel building density values 17,924 ~ 81,613).

### 2.3.4 Quantification of Cooling Intensity and Urban Green Space Characteristics

The UHI effect mitigation is related to the area, shape, and other factors of the green space<sup>[30][31]</sup>, but the mechanism leading to the optimal cooling effect has not been clearly understood, as well as the relations between the cooling intensity and the size and shape of green space<sup>[22][32]</sup>. Accordingly, assisted with SPSS 24.0, the study quantified these relations in community parks by examining green space indicators both on typological characteristics—



3-1



3-2

3. 社区公园不同距离缓冲带的地表温度变化特征。拟合曲线整体呈现先上升后下降的趋势，社区公园斑块对周围一定距离的区域有较明显的降温效果。
3. Variation characteristics of surface temperature in each buffer ring of the community park. The fitting curve shows a trend of rising first and then falling, and the park have obvious cooling effect on the surrounding area at a certain distance.

状的面积 (AREA)、紧凑度 (CI) 和景观形状指数 (LSI)，利用 ENVI 5.3 计算反映斑块生物学特征的地表温度 (LST) 和归一化植被指数 (NDVI)，并结合 SPSS 24.0 探究影响社区公园降温强度的相关影响因素之间的关系 (表 1)。

### 2.3.5 最佳降温强度与面积阈值识别

本研究使用 SPSS 24.0 对研究区域中社区公园的平均最优面积进行回归分析。研究采用余兆武等人提出的城市冷岛范围、强度和效率的

including the Area (AREA), Compaction Index (CI), and Landscape Shape Index (LSI), calculated with the ArcGIS 10.4 and FRAGSTATS—and the biological characteristics—including LST and Normalized Difference Vegetation Index (NDVI), calculated with ENVI 5.3 (Table 1).

### 2.3.5 Optimal Cooling Intensity and Threshold-Size

SPSS 24.0 was used to estimate the threshold-size for optimal cooling intensity of community parks. An assessment

阈值 (TVoE) 理论构架评估最优社区公园面积<sup>[17]</sup>: 当社区公园降温强度和面积的最优拟合曲线为对数曲线, 且TVoE位于对数斜率为1的位置时, 面积最佳, 即能达到最理想降温效果的最小公园面积。如图2—2在达到TVoE前, 降温强度会随社区公园面积的增大而迅速增加; 而一旦超过TVoE, 降温强度的提升幅度将非常有限。

### 3 研究结果与分析

#### 3.1 社区公园对周围环境的降温效果

利用ArcGIS 10.4的分区统计工具将社区公园、缓冲区, 以及反演得到的地表温度进行叠加, 提取每个公园内部的平均温度及各缓冲带内平均地表温度。以缓冲带距离为自变量, 缓冲带内平均地表温度为因变量, 用SPSS 24.0进行曲线拟合, 发现三次多项式的拟合效果最佳, 且94%的三次曲线模型的R<sup>2</sup>在0.6~1之间, 69%的三次曲线模型的R<sup>2</sup>在0.8~1之间。

本文选择拟合程度较高的4个社区公园作具体说明。如图3—1所示, 拟合曲线呈现先上升后下降趋势, 说明社区公园对一定距离内的周边区域具有较明显的降温效果。本研究中将温度拟合曲线由上升变为下降的拐点位置 (图中红点) 所对应的x轴视为每个社区公园的降温范围E<sub>max</sub>。以往研究发现背景气象条件 (降水、风速、相对湿度等) 对城市绿地降温效果有一定影响<sup>[33]</sup>, 不同方向的地表温度可能受光照、风向、风速等影响, 随缓冲带距离变化呈现不同结果。如图3—2所示, 本研究进一步选取16号社区公园东、南、西、北4个断面方向的采样点进行测绘, 发现各断面方向上的降温范围均为200m左右。此外, 16号

framework of UCI effect extent, intensity, and threshold value of efficiency (TVoE) proposed by Yu Zhaowu et al.<sup>[17]</sup> was adopted in this research: the threshold-size of a community park (i.e. the smallest area of a park that supports an optimal cooling effect) was identified when the best fitting curve of the cooling intensity and the area of community parks is a logarithmic, with the TVoE occurring at the point where the slope of the resulting logarithmic function equals 1. As shown in Figure 2-2, the cooling intensity increases rapidly as the park size enlarges before reaching the TVoE; across that, the cooling intensity little increases.

### 3 Results and Analyses

#### 3.1 The Cooling Effect of Community Parks on the Surrounding Areas

With the zonal statistical tool of ArcGIS 10.4, community parks, buffer zones, and LST were overlapped to obtain the average LST inside each park and of each buffer ring. The research used SPSS 24.0 to probe into the curve fitting degree, where the buffer ring distance was independent variable, and the average LST of buffer ring was the dependent variable. The result showed that the fitting effect of cubic polynomial was optimal, where R<sup>2</sup> valuing 0.6 ~ 1 accounted for 94%, and R<sup>2</sup> valuing 0.8 ~ 1 accounted for 69%.

4 community parks with a high fitting degree are illustrated here. All the fitting curves in the Figure 3-1 rise first and then decline, which indicates that those community parks have a significant cooling effect on the surrounding area within a certain distance. In this study, the x-axis value in accordance with the cooling extent of each community park was defined as the E<sub>max</sub>, marked in red on the curve. Existing studies have proven that the local climate conditions (precipitation, wind speed, relative humidity, etc.) may impact the cooling effect of urban green space to some extent<sup>[33]</sup>. The LST within the buffer rings is also subject to the orientation, light, wind direction and speed, etc. Specifically,

表2: 社区公园的降温范围  
Table 2: The cooling extent of community park

编号 Number	公园名称 Name of park	面积 (hm <sup>2</sup> ) Area (hm <sup>2</sup> )	降温范围 (m) Cooling extent (m)	编号 Number	公园名称 Name of park	面积 (hm <sup>2</sup> ) Area (hm <sup>2</sup> )	降温范围 (m) Cooling extent (m)
1	鼓楼市民广场 Drum Tower Civic Plaza	2.48	150 - 180	4	阳光广场 Sunshine Plaza	2.16	120 - 150
2	和平公园 Peace Park	1.61	150 - 180	5	南湖广场 South Lake Plaza	1.81	30 - 60
3	刘伯承广场 Liubo Cheng Plaza	1.33	0 - 30	6	明御河公园 Mingyu River Park	1.21	90 - 120

续表见下页 / Continued

表2: 社区公园的降温范围  
Table 2: The cooling extent of community park

编号 Number	公园名称 Name of park	面积 (hm <sup>2</sup> ) Area (hm <sup>2</sup> )	降温范围 (m) Cooling extent (m)	编号 Number	公园名称 Name of park	面积 (hm <sup>2</sup> ) Area (hm <sup>2</sup> )	降温范围 (m) Cooling extent (m)
7	光华游园 Guanghua Garden	2.58	390 - 420	30	晓山山头广场 Xiaoshan Mountain Plaze	2.43	30 - 60
8	大行宫市民广场 Daxinggong Civic Plaza	1.57	0 - 30	31	摄山社区公园 Sheshan Community Park	3.04	120 - 150
9	铁路北街广场 Railway North Street Plaza	1.57	300 - 330	32	恒茂家园游园 Hengmao Home Garden	1.69	30 - 60
10	积善广场 Moriyoshi Plaza	1.37	0 - 30	33	察哈尔路市民广场 Chahar Road Civic Plaza	1.03	30 - 60
11	月光广场 Moonlight Plaza	2.13	120 - 150	34	回龙桥社区绿地 Huilong Bridge Community Green Land	1.74	360 - 390
12	春水苑公园 Chunshuiyuan Park	1.64	150 - 180	35	兴达社区公园 Xingda Community Park	1.12	30 - 60
13	尧林仙居社区公园 Yaolinxianju Community Park	1.58	120 - 150	36	岗山桥公园 Gangshan Bridge Park	1.06	150 - 180
14	宝塔山社区公园 Baota Mountain Community Park	1.47	60 - 90	37	殷华街广场 Yinhua Street Plaza	1.50	120 - 150
15	南湾营广场 Nanwanying Plaza	2.00	0	38	水月情怀公园 Shuiyueqinghuai Park	1.67	0 - 30
16	华电西苑山体公园 Huadianxiyuan Mountain Park	9.66	180 - 210	39	牛头山社区公园 Cow Head Mountain Community Park	6.48	120 - 150
17	葛塘广场 Getang Plaza	1.36	30 - 60	40	将军大道桥头公园 General Avenue Bridgehead Park	1.02	0
18	仪凤广场 Yifeng Plaza	1.03	150 - 180	41	新城路社区公园 Xincheng Road Community Park	2.98	90 - 120
19	百家湖花园 Baijiahu Garden	1.07	120 - 150	42	龙华路街心公园 Longhua Road Central Park	1.21	90 - 120
20	竹山公园 Bamboo Mountain Park	3.04	270 - 300	43	尧和路社区公园 Yaohe Road Community Park	1.08	0 - 30
21	尧化门市民广场 Yaohuamen Civic Plaza	3.06	60 - 90	44	仙隐北路社区公园 Xianyin North Road Community Park	1.13	30 - 60
22	翠屏国际城公园 Cuiping International City park	1.39	0 - 30	45	学林路社区公园 Xuelin Road Community Park	1.84	0 - 30
23	文鼎路社区公园 Wending Road Community Park	2.45	0	46	步青路社区公园 Buqing Road Community Park	1.50	90 - 120
24	雨花台政府公园 Yuhuatai Government Park	3.51	180 - 210	47	晓庄社区公园 Xiaozhuang Community Park	1.74	30 - 60
25	花神湖公园 Huashen Lake Park	3.45	0 - 30	48	幕府山庄社区公园 Mufu Villa Community Park	1.58	0
26	永恒家园西侧公园 West Side of Eternal Home Park	1.12	120 - 150	49	学子路社区公园 Xuezi Road Community Park	5.19	90 - 120
27	雅居乐公园 Yajule Park	1.82	0 - 30	50	城市绿洲社区公园 Urban Oasis Community Park	3.13	30 - 60
28	升景坊游园 Shengjingfang Garden	2.02	30 - 60	51	下马坊社区文化广场 Xiamafang Community Cultural Plaza	1.03	0 - 30
29	九龙公园 Nine Dragon Park	2.16	150 - 180	52	紫东路社区公园 Zidong Road Community Park	1.23	30 - 60

4. 量化社区公园降温强度随距离变化的特征发现, 降温强度随缓冲带距离的增加而逐渐减小, 总体趋于0。
4. It is found that the cooling intensity decreases with the increase of buffer ring distance and approaches 0°C in the end.

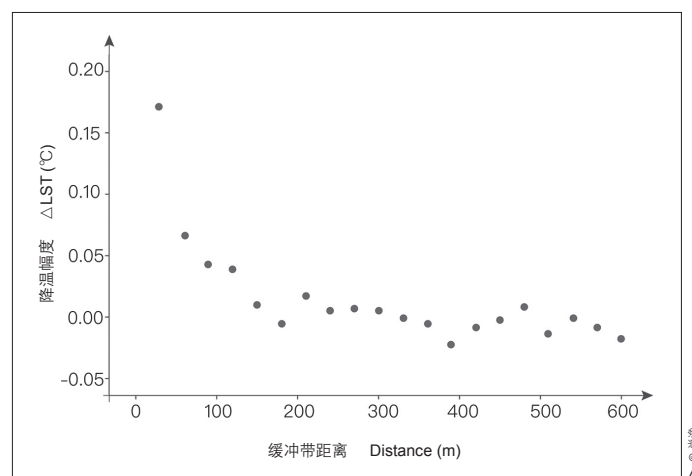
社区公园的东、南、北三个断面方向上的地表温度变化幅度与图3-1也基本一致, 西断面地表温度走势与其余三个方向略有不同。这是由于16号社区公园西侧约400m处有一个降温效果良好的城市专类公园(红山森林动物园), 因此, 其西断面的地表温度走势在300m之外随缓冲区距离的增大而逐渐下降。

从表2可以看出, 社区公园的降温范围集中于0~180m(涵盖46个社区公园), 平均降温范围为90~120m。其中, 15号、23号、40号、46号以及48号由于公园内下垫面硬质率过大, 或缓冲区内存在较大水体、绿地而不具备明显降温效果。

研究进一步量化社区公园降温强度随距离变化的特征, 计算得到公园各个缓冲带之间的平均温差(简称缓冲带降温幅度)。社区公园内部较外侧30m缓冲带降温幅度最显著, 为0.187°C; 0~30m缓冲带较30~60m缓冲带降温幅度为0.075°C, 降温效果有所减弱。总体而言, 随着缓冲带距离增加, 降温强度逐渐减小; 缓冲带距离超过300m时, 社区公园降温效果几乎消失, 同时受到周边环境干扰, 降温强度开始在0°C上下波动(图4)。

### 3.2 降温强度的相关影响因素

本研究中52个社区公园的降温强度范围为0~2.612°C, 平均值为0.604°C, 降温强度的显著变化证实了景观特征的空间异质性<sup>[34]</sup>。利用SPSS 24.0进一步计算5个形状特征因子与降温强度间的相关系数(图5), 为避免误差, 计算中去除了个别异常值(如25号社区公园, 其形状指数远大于其他社区公园)。结果表明, NDVI ( $R=0.354$ ,  $p<0.01$ )、AREA ( $R=0.467$ ,  $p<0.001$ )、CI ( $R=0.403$ ,  $p<0.001$ )与降温强度呈正相关, 公园温度(P\_LST) ( $R=-0.683$ ,  $p<0.001$ )和LSI ( $R=-0.393$ ,  $p<0.001$ )与降温强度呈负相关, 即当社区公园在一定阈值范围内具有更高的NDVI、更大的面积, 以及更规则的形状时, 其降温效果最佳, 该结论与已有研究结论一致<sup>[28][35]</sup>。鉴于当前欠缺不同核建筑密度下社区公园的最佳面积阈值和形状规律的相关研究, 本文进一



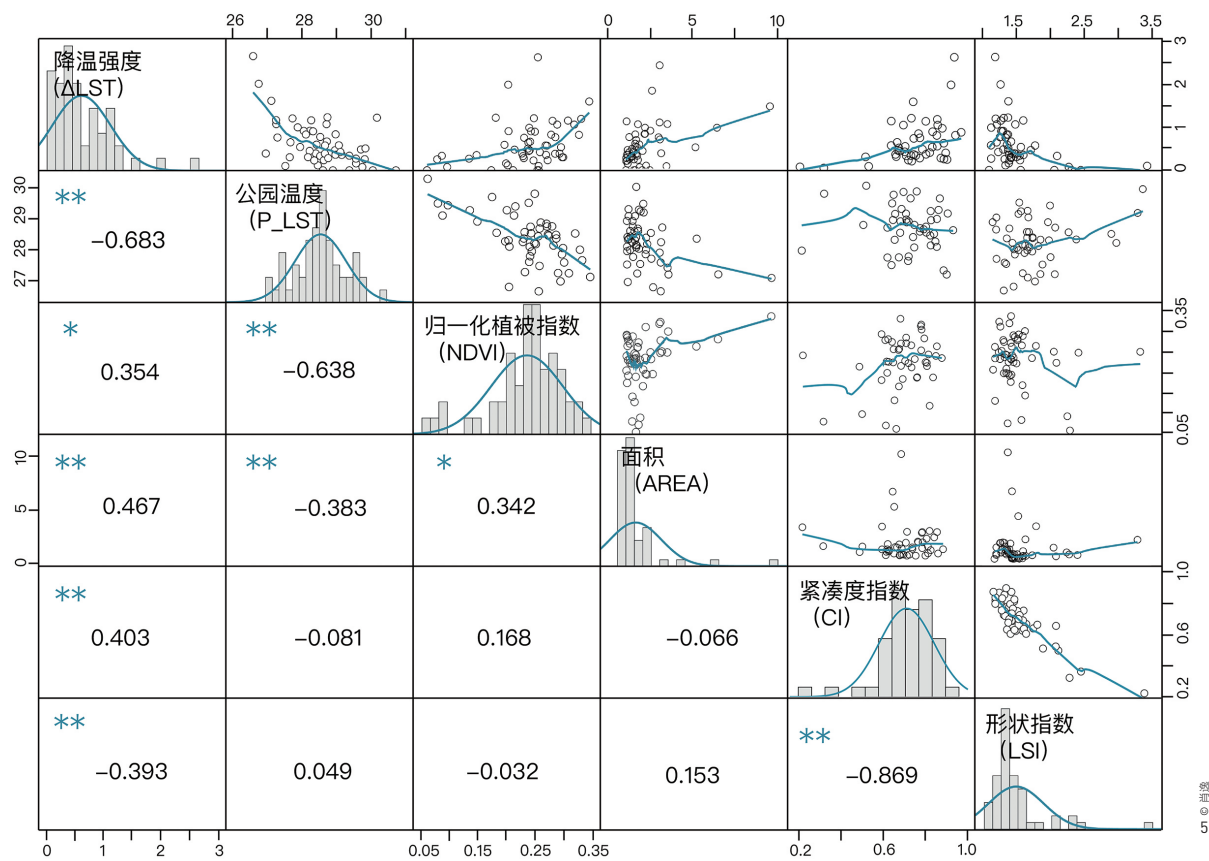
the study further surveyed and mapped the sampling points in the east, south, west, and north of No. 16 park, and found the  $E_{max}$  in each section was about 200 m (Fig. 3-2). In addition, the variation of LST in the east, south, and north section was consistent with its overall fitting curve; the LST variation in the west section was slightly different because of its proximity to an urban park (sitting 400 meters from the Hongshan Forest Zoo) that had a significant cooling effect on the No. 16 park, leading to a decrease of LST in the west section beyond 300 meters.

The  $E_{max}$  of community parks are mostly less than 180 m (46 parks), with an average cooling extent of 90 ~ 120 m. Among them, the parks of No.15, No.23, No.40, No.46, and No.48 contributed little to the cooling effect on the surrounding areas, mostly on account of their high ratio of impervious surface, or large-sized water bodies or green spaces in their buffer zones (Table 2).

To further quantify the variation of cooling intensity of each community parks on the surrounding areas, the average LST difference between each buffer ring of the park was obtained (called the cooling intensity of buffer ring). The cooling intensity difference between the inner park and the first buffer ring was 0.187°C; the difference between the first and the second was 0.075°C. Overall, with the increase of the buffer ring distance, the cooling intensity decreases; the cooling intensity difference was barely found when the distance exceeds 300 meter, which would slightly fluctuate around 0°C due to the impacts from the surrounding environment (Fig. 4).

### 3.2 Cooling Intensity and Urban Green Space Characteristics

The cooling intensity of the 52 community parks ranged from 0°C to 2.612°C, with an average of 0.604°C—the significant cooling effect verifies the spatial heterogeneity shaped by the typological characteristics of landscapes<sup>[34]</sup>. The correlation coefficients between the 5 typological indicators and cooling intensity were calculated with SPSS 24.0 (Fig. 5), where individual outliers were eliminated (for instance, the shape index of No.25 park was far larger shape than the others). The results showed that the cooling intensity was positively correlated with NDVI ( $R = 0.354$ ,  $p < 0.01$ ), AREA ( $R = 0.467$ ,  $p < 0.001$ ), CI ( $R = 0.403$ ,  $p < 0.001$ ) while negatively correlated with the land surface temperature of park (P\_LST) ( $R = -0.683$ ,  $p < 0.001$ ) and LSI ( $R = -0.393$ ,  $p < 0.001$ ). In other word, within the thresholds, the cooling effect of a community park can be optimized with a larger size, a higher NDVI, and in a more regular shape, which is consistent with other research findings<sup>[28][35]</sup>. Originally, this research further examined the threshold-size and optimal shape of community parks under



注  
\*表示P<0.01, \*\*表示P<0.001。

NOTE  
\*: P < 0.01; \*\*: P < 0.001.

- 利用SPSS 24.0计算了5个社区公园的形状特征因子与降温强度之间的相关系数, 结果表明, 降温强度与NDVI、AREA、CI均显著正相关。
- The correlation coefficients between 5 typological characteristic factors of community parks and cooling intensity were calculated by SPSS 24.0. The results showed that cooling intensity was positively correlated with NDVI, AREA, and CI.

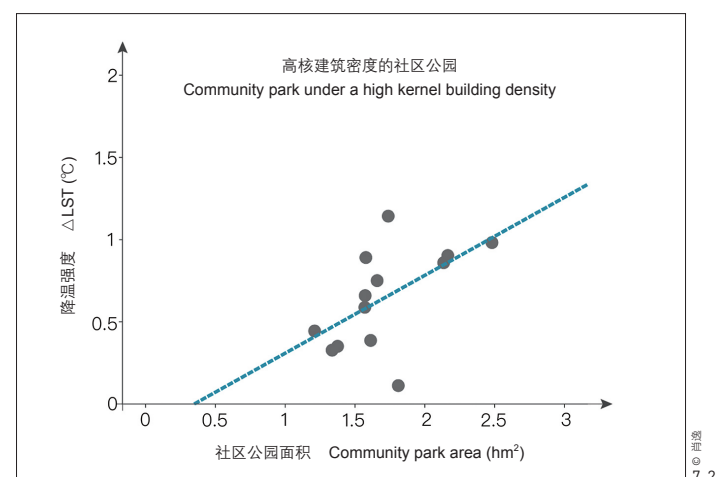
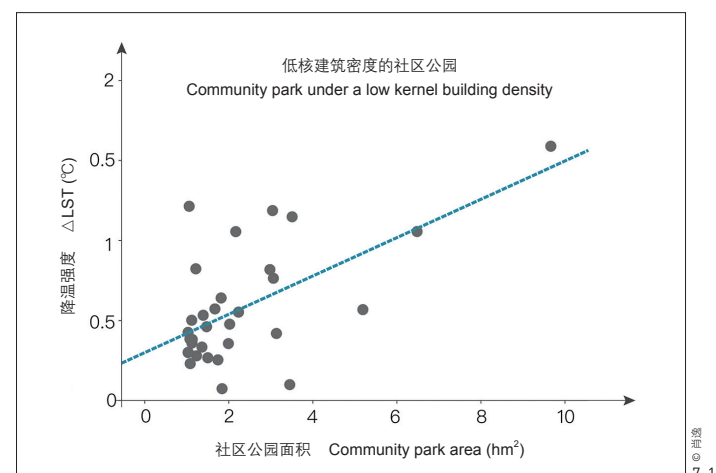
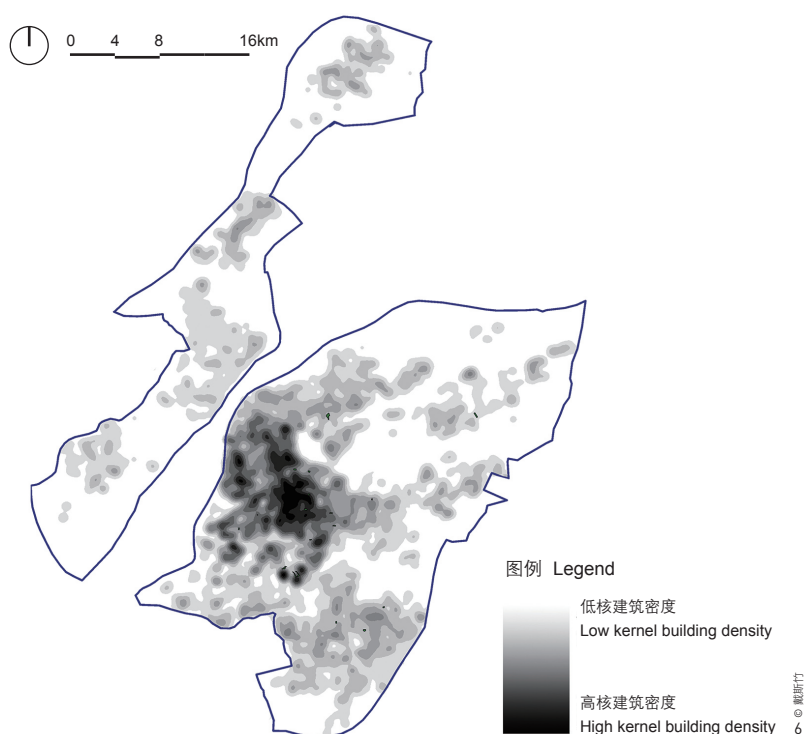
表3: 不同核建筑密度下社区公园降温强度与相关影响因素分析  
Table 3: Analysis of cooling intensity and the causal factors in community parks under different kernel building densities

类别 Type	数量 (个) Number (piece)	平均面积 (hm <sup>2</sup> ) Mean area (hm <sup>2</sup> )	平均降温强度 (°C) Mean intensity (°C)	平均紧凑度指数 Mean CI	平均形状指数 Mean LSI	平均归一化植被指数 Mean NDVI
社区公园 Community park	52	2.114	0.604	0.734	1.481	0.253
高核建筑密度的社区公园 Community park under a high kernel building density	14	1.773	0.741	0.738	1.409	0.239
低核建筑密度的社区公园 Community park under a low kernel building density	38	2.239	0.532	0.721	1.508	0.258

步计算了高、低核建筑密度类型的社区公园的相关影响因素的平均值 (表3)。其中, 低核建筑密度的社区公园平均降温强度为0.554°C, 高核建筑密度的社区公园平均降温强度为0.741°C, 两者相差0.187°C; 高核建筑密度的社区公园具有较为规整的形状特征, 但公园面积和NDVI略小于低核建筑密度的社区公园。

different kernel building density types (Table 3): the average cooling intensity of community parks under a low kernel building density was 0.554°C, and 0.741°C for the ones under a high kernel building density—the intensity difference was 0.187°C; Compared with the community parks under a low kernel building density, the parks under a high kernel building density were found in a more regular shape, but slightly lower in AREA and NDVI.

6. 南京市中心城区高、低核建筑密度分级图
7. 高、低核建筑密度的社区公园的降温强度与面积相关分析
6. Distribution of kernel building density in the central area of Nanjing
7. Correlation analysis of cooling intensity and area of community parks under high and low kernel building density



### 3.3 社区公园的最佳面积阈值

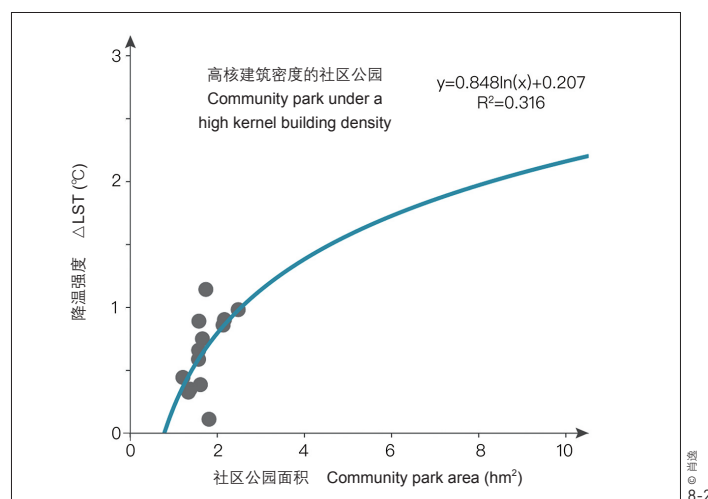
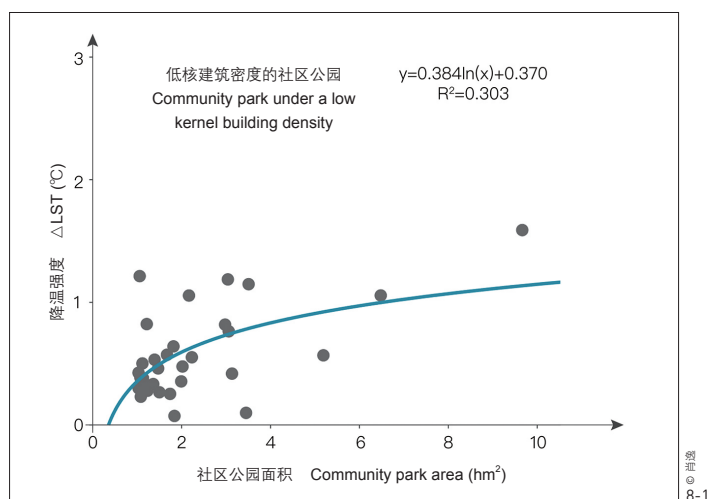
本研究所分析的52个社区公园面积为1.019~9.663hm<sup>2</sup>不等，尽管面积与降温强度呈正相关，但部分社区公园面积较小，降温强度不显著，主要是当公园较小时易受其他因素影响（如位置、周围环境等），如45号社区公园面积为1.84hm<sup>2</sup>，其自身下垫面硬质率偏高且毗邻风景区。此外，低、高核建筑密度的社区公园的面积和降温强度间的变化关系存在显著差异（图6，7）。通过线性拟合发现（计算中去除个别异常值），在本研究中，低核建筑密度的社区公园斜率为0.12（ $R^2=0.369$ ， $p<0.001$ ），高核建筑密度的社区公园斜率为0.51（ $R^2=0.501$ ， $p<0.01$ ），更加表明高核建筑密度的社区公园对周边环境降温效果更为显著。

接着，利用SPSS 24.0对社区公园的面积与降温强度进行一元线性回归分析，结果显示二者呈对数函数关系（图8），发现低核建筑密度的社区公园（ $R^2=0.303$ ， $p<0.01$ ）和高核建筑密度的社区公园

### 3.3 The Threshold-Size of Community Parks

The size of the 52 parks ranged from 1.019 to 9.663 hm<sup>2</sup>. Although this research found that the size of the parks was positively correlated with their cooling intensity, the insignificant cooling intensity observed in smaller parks was also resulted from location reasons or the impacts by their surrounding environments. For instance, the No.45 park (1.84 hm<sup>2</sup>) has a high impervious surface ratio and is adjacent to a large-scale green space (a scenic area). In addition, this correlation was strongly impacted by the kernel building density of the community parks (Fig. 6, 7). The linear fitting analysis (outliers removed) revealed that the slope of community parks under a low kernel building density was 0.12 ( $R^2 = 0.369$ ,  $p < 0.001$ ), and 0.51 ( $R^2 = 0.501$ ,  $p < 0.01$ ) for the parks under a high kernel building density, evidencing that the latter ones had a more significant cooling effect on the surrounding areas.

Through a simple linear regression to analyze the size and the cooling intensity of community parks with SPSS 24.0, the logarithmic function relation between those two was identified (Fig. 8). As the area of the parks increases, the cooling intensity under the both density



8. 高、低核建筑密度的社区公园降温强度和面积阈值的分析表明：高核建筑密度的社区公园的最佳面积阈值为0.423hm<sup>2</sup>，“低”的为0.376hm<sup>2</sup>。
8. According to the analysis of cooling intensity and the threshold-size of community parks under high and low kernel building density, the threshold-size of community parks under a high kernel building density is 0.423 hm<sup>2</sup>, and 0.376 hm<sup>2</sup> for the parks under a low kernel building density.

( $R^2=0.316$ ,  $p<0.05$ ) 的降温强度随着公园面积的增大而逐渐趋于平缓、稳定。但对应的最佳公园面积阈值存在显著差异：低核建筑密度的社区公园，最佳阈值为0.384hm<sup>2</sup>；高核建筑密度的社区公园，阈值远大于前者，为0.848hm<sup>2</sup>。

### 3.4 社区公园的最优形状规律

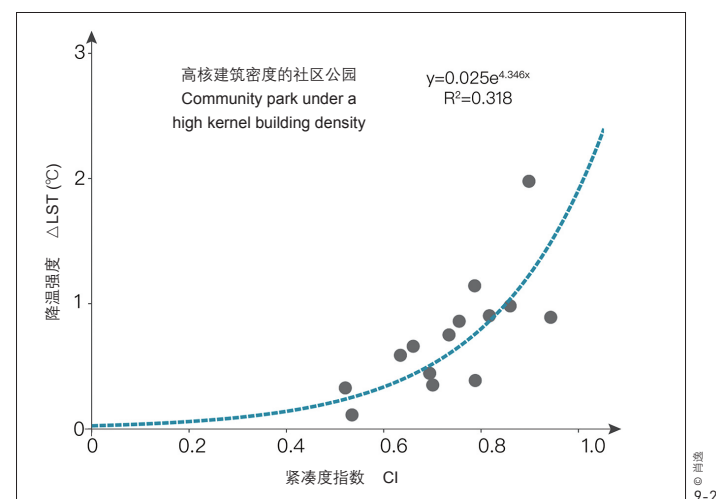
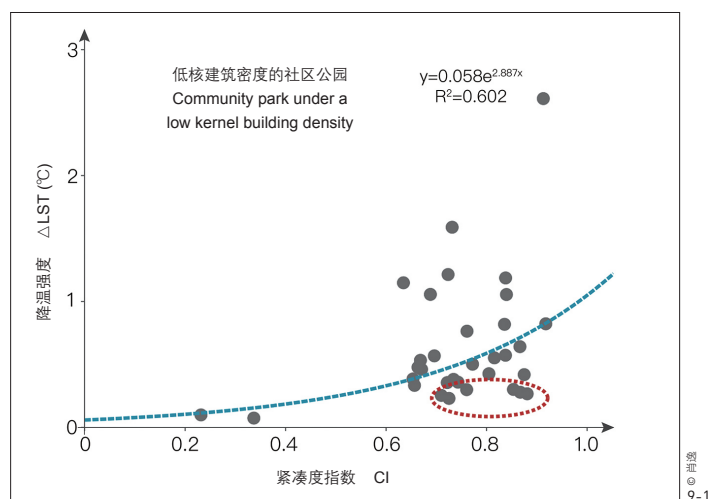
紧凑度指数被用于测度景观形状特征，研究选择圆形率紧凑度分析社区公园形状规律。经测算发现，社区公园的紧凑度指数与降温强度为指数函数，呈正相关 ( $R=0.434$ ,  $p<0.05$ )，当CI值接近1时，即公园趋于圆形或正方形时，降温效果最显著，该结论与多数既有研究结论一致<sup>[36][37]</sup>。如图9所示，低核建筑密度的社区公园拟合性较弱 ( $R^2=0.318$ ,  $p<0.01$ )，高核建筑密度的社区公园拟合性较强 ( $R^2=0.602$ ,  $p<0.001$ )。但受限于较少的研究样本数量，难以对该关系形成有效验证，如图9-1中，有较多散点分布于拟合曲线下方。研究进一步验证发现，这些散点对应的社区公园多是由于自身NDVI值过小，或社区公园受周边环境影响较大。如37号社区公园的CI值为0.881，而其降温强度仅为0.267℃，多由于其自身下垫面硬质率较高且NDVI值较低（仅为0.169，远小于平均值0.239）所致；18号社区公园的CI值和NDVI值均较高，但其降温强度也仅为0.301℃，这是由于该公园

types of community parks soars first and then stays at a certain extent (the one under a low kernel building density:  $R^2 = 0.303$ ,  $P < 0.01$ ; the one under a high kernel building density:  $R^2 = 0.316$ ,  $P < 0.05$ ). However, the threshold-size of community parks under the both density types showed a significant difference: 0.384 hm<sup>2</sup> for the parks under a low kernel building density and 0.848 hm<sup>2</sup> for the ones under a high kernel building density.

### 3.4 The Optimal Shape of Community Parks

The circularity ratio of CI, a metric to the shape characteristic of a landscape, was selected to analyze the shape factor of community parks. It showed that the CI and their cooling intensity of the studied parks was an exponential function with positive correlation ( $R = 0.434$ ,  $p < 0.05$ ), and the optimal cooling effect would occur when CI value was close to 1 (i.e. the park in a shape of circle or square), being consistent with most existing studies<sup>[36][37]</sup>. As shown in the Figure 9, community parks under a low kernel building density had a lower fitting degree ( $R^2 = 0.318$ ,  $p < 0.01$ ), compared to the ones under a high kernel building density ( $R^2 = 0.602$ ,  $p < 0.001$ )— However, these fitting correlations need to be further verified because of the limited samples in this study, most of which were scattering below the fitting curve (Fig. 9-1). The reason for this fitting pattern was that the NDVI value of the corresponding parks was extremely low, or those parks were affected by the surrounding environments. For instance, the CI value of No.37 park was 0.881 and its cooling intensity was only 0.267℃, might resulting from its high impervious surface ratio and low NDVI value (NDVI = 0.169, far less than the average level); The No. 18 park had both high CI and NDVI values but a very low cooling intensity (0.301℃), probably because of the park's

9. 社区公园的降温强度和紧凑度指数呈正相关。
9. There is a positive correlation between the cooling intensity and CI of community parks.



北部紧邻大型风景区，南部则靠近较大的城市公园（内含水体），周边环境的降温强度更显著，降温范围对18号社区公园造成较大影响。

此外，相关研究表明城市蓝绿空间的形状规律存在阈值大小：当面积大于1hm<sup>2</sup>时，即使形状复杂也能起到较好的降温效果<sup>[38]</sup>。这与本研究结论略有偏差，主要原因是对于社区公园而言，其面积普遍较小，多为1~4hm<sup>2</sup>，而形状越不规则的公园与周边环境的交界面越大，会使更多冷空气从本来面积就已很小的绿地中输送出去；而对于大面积的蓝绿空间而言，其更易产生相对独立的局部小气候<sup>[32][39]</sup>。因此，形状复杂性对面积较小的社区公园的降温效果影响更大。

## 4 讨论

### 4.1 影响社区公园降温范围的因素

针对南京市社区公园冷岛效应的影响范围和降温强度分析，52个公园降温范围多集中于0~180m，平均降温范围114.23m，平均降温强度0.604℃。另外，7号社区公园、9号社区公园，以及34号社区公园的降温范围超过300m，均属于高核建筑密度类型（表4）。其中34号社区公园以林地为主，NDVI值为同类别最高。哈希姆·阿克巴里等人发现，不同的绿地结构会显著影响城市冷岛效应，当城市景观的植被茂密且生长健康时，降温效果更显著，且以林地为主的绿地降温效果优于草地类型<sup>[40]</sup>，该结论解释了34号社区公园具有较高降温范围的情况。而7号社区公园和9号社区公园临水，它们的降温强度和范围远高于同类别相似环境的3号社区公园。研究分析造成这一差异的原因可能有以下三

adjacency to a large scenic area in the north and a bigger urban park (covering water bodies) in the south, which two impacted the park's cooling intensity considerably.

Besides, relevant studies on urban blue-green spaces have also demonstrated that when a park's size exceeds 1 hm<sup>2</sup>, its cooling effect would be little subject to whatever the park's shape is<sup>[38]</sup>, which is deviated from the findings of this study. Compared to larger blue-green spaces that can form a relatively local micro-climate, community parks (mostly being 1 ~ 4 hm<sup>2</sup>) would have a poorer cooling effect if they are in an irregular shape, due to the increased inner-outer interface would lead to more diffuse thermal flows<sup>[32][39]</sup>. In this sense, the shape irregularity has greater impact on the cooling effect of smaller community parks.

## 4 Discussions

### 4.1 Causal Factors to the Cooling Extent of Community Parks

In this research, the main findings on the cooling extent and intensity of community parks in central area of Nanjing—including the cooling extent of the 52 studied community parks was mostly less than 180 meters, the average cooling extent of 114.23 meter, and the average cooling intensity was 0.604℃—verify existing research outcomes. Remarkably, the cooling extent of the No.7, No.9, and No.34 community parks exceeded 300 meters, all of which were under a high kernel building density (Table 4). Specifically, the No.34 community park was mostly occupied with woodland and it had the highest NDVI value among the parks under a high kernel building density. The study by Hashem Akbari et al. explained that green spaces' structure can largely define their UCI effect: the more healthy and denser vegetation an urban landscape is occupied, a more significant

表4: 3号、7号、9号和34号社区公园的降温范围与相关影响因素  
Table 4: The cooling extent and the causal factors in No. 3, 7, 9, and 34 community parks

编号 Number	公园名称 Name of park	面积 (hm <sup>2</sup> ) Area (hm <sup>2</sup> )	降温强度 (°C) Cooling intensity (°C)	形状指数 LSI	归一化植被指数 NDVI	降温范围 (m) Cooling extent (m)
3	刘伯承广场 Liubo Cheng Plaza	1.336	0.328	2.079	0.249	0 - 30
7	光华游园 Guanghua Garden	2.585	1.978	1.240	0.227	390 - 420
9	铁路北街广场 Railway North Street Plaza	1.573	0.660	1.396	0.259	300 - 330
34	回龙桥社区绿地 Huilong Bridge Community Green Land	1.738	1.143	1.243	0.292	360 - 390

点: 1) 3号社区公园相对7号社区公园和9号社区公园面积较小且形状复杂, 导致公园整体降温强度较弱; 2) 3号社区公园以草地为主, 而7号社区公园和9号社区公园以林地为主, 以林地为主的公园不仅能更有效地降温, 同时对改善区域空气质量和提供其他生态系统服务具有重要作用<sup>[31][41]</sup>; 3) 由于7号和9号社区公园都与周边绿地及水体相连, 形成完整的带状空间, 该结构一定程度上能有效降低地表温度, 具有较高的降温强度和降温范围<sup>[11][13]</sup>, 这也从侧面佐证了“水体是影响冷岛效应的重要因素”的相关研究结论<sup>[38][42]</sup>。

#### 4.2 基于核建筑密度的社区公园模式分类

研究根据社区公园周边核建筑密度分布的差异性, 将52个社区公园分为高、低两种核建筑密度类型。低核建筑密度的社区公园多位于城市核心区周边, 公园的最佳面积阈值为0.384hm<sup>2</sup>, 平均降温强度为0.532°C; 高核建筑密度的社区公园多位于城市核心区以内, 公园的最佳面积阈值为0.848hm<sup>2</sup>, 平均降温强度达0.741°C, 而该面积阈值远大于低核建筑密度的社区公园, 主要是因为核建筑密度越高, 建成区城市热岛效应更加明显, 而较大的绿地更有利于达到最佳降温效果<sup>[14][39]</sup>。

分析表明, 两种类型社区公园的降温强度均易受周边环境的影响。通过提取52个社区公园周边0~600m缓冲区的NDVI发现, 高核建筑密度的社区公园缓冲区内平均NDVI值为0.149, 低核建筑密度的社区公园缓冲区内平均NDVI值为0.184 (图10)。综合考虑公园自身和周边环境, 在其他影响因素相同条件下, 高核建筑密度的社区公园相比低核建筑密度的社区公园, 需要更大的公园面积才能达到最佳降温效果。

cooling effect it has, where woodland landscapes show a better cooling effect than grasslands<sup>[40]</sup>. The parks of No. 3, No. 7, and No.9 are close to water areas, but the cooling intensity and extent of both the latter two parks were far higher than the No. 3 park. The possible reasons are as follows: 1) compared with No. 7 and No. 9, No. 3 park covers a smaller area and is in more complex shape, which would weaken the cooling intensity of the park; 2) No. 3 park is covered by grasslands, and No. 7 and No. 9 parks by woodland which can not only cool the air more efficiently but also provide other ecosystem services such as improving air quality<sup>[31][41]</sup>; and 3) No. 7 and No. 9 are connected with surrounding water and green spaces together forming a larger green space that would perform a stronger cooling intensity and a wider cooling extent<sup>[11][13]</sup>—this also corroborates the study conclusions that water body is an important causal factor to UCI effect<sup>[38][42]</sup>.

#### 4.2 Community Park under Different Kernel Building Densities

The 52 studied community parks were identified under different kernel building densities. Most parks under a low kernel building density locate around the central area of the city, and the threshold-size of such parks was 0.384 hm<sup>2</sup> and the average cooling intensity was 0.532°C. The parks under a high kernel building density are mostly sitting within the central area of the city, with the threshold-size as 0.848 hm<sup>2</sup> and 0.741°C for the average cooling intensity. The disparity of threshold-size was caused by the fact that the heavier UHI effect of urban built-up areas under a high kernel building density can only be efficiently mitigated by a green space that covers a large-enough area<sup>[14][39]</sup>.

It was found that the cooling intensity of the parks under both kernel building densities were easily impacted by the environmental factors from the surrounding areas. An across-examination on the NDVI value of 0 ~ 600 m buffer zone of each park indicated that

10. 高、低核建筑密度的社区公园面积及其周边0-600m缓冲区的NDVI示意图

10. Scheme of the NDVI of 0-600 m buffer zones around 52 community parks under high and low kernel building density and their areas

该结论可能是受限于高核建筑密度的公园样本量过少,且公园面积集中在1.2~2.6hm<sup>2</sup>所致(表3)。

#### 4.3 城市绿地系统规划层面的指标调整建议

本研究试图探讨最佳降温效果下社区公园的面积阈值和形状规律。研究发现,南京市社区公园的面积、形状、NDVI和降温强度显著相关,且低核建筑密度和高核建筑密度的社区公园最佳面积阈值分别为0.384hm<sup>2</sup>和0.848hm<sup>2</sup>,均小于《城市绿地分类标准(2017)》对社区公园“宜超过1hm<sup>2</sup>”的规定。因此,建议根据各地区城市的实际情况,在城市绿地系统规划层面适当调整社区公园绿地面积指标,有助于在高核建筑密度地块内见缝插针地规划小面积绿地,利用精细化的存量设计与管理,发挥城市区域的最佳生态效益,进一步缓解局部热岛效应。同时,将基于自然的解决方案和生态设计等理念纳入城市规划和管理体系,有利于在快速城镇化过程中有效应对环境压力与挑战。

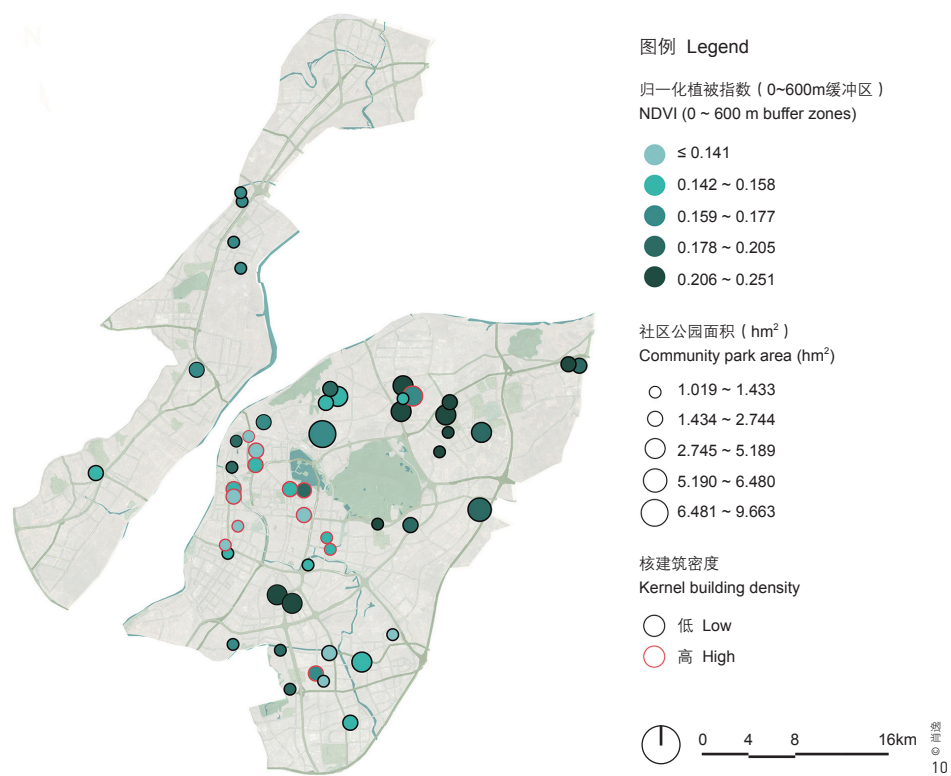
针对本研究范围而言,低核建筑密度的社区公园具有面积较大,NDVI平均值较高等特征。为了营造更加舒适的公园内部热环境,在绿地布局时,应注重对现有植被生境的保护和恢复,合理构建新的植被群落。条件允许时,可通过丰富公园内绿植层次与规模来获得最佳冷岛效应,并将较零散的绿地进行整合。城市核心区内的社区公园多为高核建筑密度,且易受周边灰色基础设施的影响。因此,在用地有限的情况下,应在城市核心区内增加社区公园等小面积绿地,同时增加社区公园

the average NDVI value of the parks under a high kernel building density was 0.149 and 0.184 for the parks under a low kernel building density (Fig. 10). Under the same factor conditions of the community parks and their surrounding environments, the parks under a high kernel building density expect a relatively larger size to support the optimal cooling effect, compared with the ones under a low kernel building density. However, this finding needs to be further verified because the number of the studied samples for the high kernel building density type is inadequate and the spectrum of park size is relatively narrow (mostly 1.2 ~ 2.6 hm<sup>2</sup>) (Table 3).

#### 4.3 Suggestions on Index Adjustment in Urban Green Space System Planning

This paper delved into the threshold-size and optimal shape of community parks that support the best cooling effect, and found that the area, shape, and NDVI of the parks were significantly correlated with their cooling intensity, wherein the threshold-size of parks under a low and high kernel building density were 0.384 hm<sup>2</sup> and 0.848 hm<sup>2</sup> respectively. Both of them are smaller than the expected size of community parks (no less than 1 hm<sup>2</sup>) by the Standard for Classification of Urban Green space (2017). Proper adjustments on the green space index in community parks of urban green space system planning should be taken according to locality conditions. Particularly, it is conducive to plan small green spaces in the areas under a high kernel building density, giving full play to the ecological benefits of urban green spaces in mitigating the local UHI effect through renewal design and refined management measures. Embracing the ideas such as Nature-Based Solutions and ecological design, urban planning and management will perform a stronger capacity to address the challenges in the rapid urbanization.

In this research, the studied community parks under a low kernel building density have a larger average size and a higher average NDVI value. To create a more comfortable micro-climate in urban parks, park designers and managers should pay attention to the protection and restoration of existing vegetation habitats and the establishment of new plant communities. The best UCI effect can be obtained by enriching the vegetation structures and scales and improving the connectivity of the green spaces within the park. Community parks within central urban areas are often under a high kernel building density and prone to the environmental impacts by grey infrastructures in the surroundings. In this sense, under the inventory planning background, the cooling effect of community parks in central areas can be improved by adding more small-scale green spaces, increasing the compactness of parks—making the parks in a more regular shape—and enhancing the



的紧凑度,使公园形状更为规则,并适当提高植被郁闭度和连续性,提升公园的降温效果。

#### 4.4 研究贡献与展望

本研究分析了南京市中心城区52个社区公园对城市热岛效应的缓解作用,探究了小尺度公园在最佳降温效果下的面积阈值与形状规律,研究成果具备一定的普适性。

研究尚有一定不足。首先,受限于研究样本与方法,本文以林地为主的社区公园占80%以上,缺少对包含水体社区公园的研究,尚未进一步展开探讨草地、灌木、乔木等具体覆被类型对于热岛效应缓解作用差异;其次,虽然本文在数据来源和研究对象的选择上尽量规避了气象等因素对温度的影响,但根据以往研究发现,气象背景条件(降水、风速、相对湿度等)对绿地的降温效果有显著影响<sup>[17][40]</sup>,因此,研究对以上气象背景条件的综合效应探论仍显不足;再次,对于社区公园降温强度的季节和昼夜差异、不同气候带和人文地理特征下的空间分异等问题也有待进一步研讨。因此,基于不同城市的研究还需考虑地域、季节、气象等背景因素的影响。

## 5 结论

本文基于遥感影像、ArcGIS及统计学工具与方法,通过分析南京市中心城区社区公园与降温强度的相关影响因素,探讨缓解城市热岛效应的最佳社区公园面积阈值和形状规律。研究得到如下结论:

1)通过对样本社区公园建立缓冲区、构建公园与周边环境温度变化的三次多项式定量模型,发现随着缓冲带距离的增加,降温强度逐渐减小,并最终趋于0℃。

2)在社区公园降温强度的影响因素中,降温强度与NDVI ( $R=0.354$ ,  $p<0.01$ )、AREA ( $R=0.467$ ,  $p<0.001$ )和CI ( $R=0.403$ ,  $p<0.001$ )呈正相关,与公园温度 ( $R=-0.683$ ,  $p<0.001$ )和LSI ( $R=-0.393$ ,  $p<0.001$ )呈负相关。表明当社区公园在一定范围内具有更大的面积、更高的NDVI以及更规则的形状时,其降温效果最佳。

3)在不同核建筑密度的社区公园最佳降温强度方面,低核建筑密度的社区公园面积阈值为 $0.384\text{hm}^2$ ,高核建筑密度的社区公园面积阈值为 $0.848\text{hm}^2$ 。

density and continuity of vegetation communities.

#### 4.4 Research Significance and Prospects

By analyzing the mitigation of 52 community parks on UHI effect in central area of Nanjing, this study explored the threshold-size and optimal shape of small-scale parks for the best cooling intensity. The research results are of certain universality.

Some limitation still exists. First, for the limited samples and research methods, more than 80% of the studied community parks are covered with woodland without water bodies, no further discussion on the difference of mitigation of the specific cover types (e.g. grass, shrub, and arbor forest) on the UHI effect; Second, previous studies have proved that meteorological conditions (precipitation, wind speed, relative humidity, etc.) strongly impact the cooling effect of green space<sup>[17][40]</sup>, which were almost avoided in this study without further probe; Third, as a supplement, focusing on the seasonal and diurnal differences in the cooling intensity, the spatial differences under different climatic zones, and cultural-geographical characteristics are also expected. For cases in different cities, it also needs to take into account the impact of regional, seasonal, meteorological, and other factors in future studies.

## 5 Conclusions

Based on the tools and methods of remote-sensing, ArcGIS, and statistics, this study analyzed the interconnection between cooling intensity and the characteristics of community parks in the central area of Nanjing, and discussed the threshold-size and optimal shape mitigating the UHI effect. Main research findings include:

1) By setting buffer zones for 52 community parks and studying cubic polynomial fitting curve between P\_LST and the average LST of buffer zone, it found that with the increase of buffer zone distance, the cooling intensity gradually decreased and tended to 0℃ in the end.

2) Among the impact factors, the cooling intensity of the community parks was positively correlated with NDVI ( $R = 0.354$ ,  $p < 0.01$ ), AREA ( $R = 0.467$ ,  $p < 0.001$ ), CI ( $R = 0.403$ ,  $p < 0.001$ ) while negatively correlated with P\_LST ( $R = -0.683$ ,  $p < 0.001$ ) and LSI ( $R = -0.393$ ,  $p < 0.001$ ). Thus, within the thresholds, the cooling effect of a community park can be optimized with a larger size, a higher NDVI, and in a more regular shape.

3) With the optimal cooling intensity under different kernel building densities, the threshold-size of community park under low and high kernel building density was  $0.384\text{hm}^2$  and  $0.848\text{hm}^2$ , respectively.

4) 采用圆形率紧凑度分析社区公园的形状特征, 其紧凑度指数与降温强度的关系符合指数函数, 公园趋于圆形或正方形 (CI趋于1) 时, 降温效果最为显著。LAF

4) Analyzing the shape characteristics of community parks with circularity ratio of CI, it showed that the relation between CI and their cooling intensity can be expressed as an exponential function, the optimal cooling effect would occur when CI value was close to 1 (i.e., the park in a shape of circle or square). LAF

## REFERENCES

- [1] United Nations Department of Economic and Social Affairs. (2018). World Urbanization Prospects 2018. Retrieved from <https://population.un.org/wup/Publications/Files/WUP2018-Highlights.pdf>
- [2] Zhou, W., Wang, J., & Cadenasso, M. L. (2017). Effects of the spatial configuration of trees on urban heat mitigation: A comparative study. *Remote Sensing of Environment*, (195), 1-12. <https://doi.org/10.1016/j.rse.2017.03.043>
- [3] Lafortezza, R., Chen, J., Van Den Bosch, C. K., & Randrup, T. B. (2017). Nature-based solutions for resilient landscapes and cities. *Environmental research*, (165), 431-441. doi:10.1016/j.envres.2017.11.038
- [4] Ordóñez, C. (2019). Polycentric Governance in Nature-Based Solutions: insights from Melbourne Urban Forest Managers. *Landscape Architecture Frontiers*, 7(3), 46-61. <https://doi.org/10.15302/J-LAF-1-020001>
- [5] Nesshöver, C., Assmuth, T., Irvine, K. N., Rush, G. M., Waylen, K. A., Delbaere, B., ... Wittmer, H. (2017). The science, policy and practice of nature-based solutions: An interdisciplinary perspective. *Science of the Total Environment*, (579), 1215-1227. <https://doi.org/10.1016/j.scitotenv.2016.11.106>
- [6] Liu, J., Lin, T., Zhao, Y., Lin, M., Xing, L., Li, X., ... Ye, H. (2019). Research progress on Nature-Based Solutions towards urban sustainable development. *Acta Ecologica Sinica*, 39(16), 6040-6050. doi:10.5846/stxb201812042648
- [7] Yu, Z., Yang, G., Zuo, S., Jørgensen, G., Koga, M., & Vejre, H. (2020). Critical review on the cooling effect of urban blue-green space: A threshold-size perspective. *Urban Forestry and Urban Greening*, (49), 126630. <https://doi.org/10.1016/j.ufug.2020.126630>
- [8] Yue, X., Lin, J., & Yang, Y. (2018). Mitigation Role of Urban Green Space in Reducing Heat Island Effect—A Case Study of Central Urban Area of Baoding City. *Landscape Architecture*, 25(10), 66-70. doi:10.14085/j.fjyl.2018.10.0066.05
- [9] Zhang, C., Xie, G. Lu, C., Liu, C., Li, N., Wang, S., & Wang, Y. (2015). The mitigating effects of different urban green lands on the heat island effect in Beijing. *Resources Science*, 37(6), 1156-1165.
- [10] Amani-Beni, M., Zhang, B., Xie, G. -D., & Shi, Y. (2019). Impacts of Urban Green Landscape Patterns on Land Surface Temperature: Evidence from the Adjacent Area of Olympic Forest Park of Beijing, China. *Sustainability*, 11(2), 513. doi:10.3390/su11020513
- [11] Du, H. (2018). The cool island effect of urban blue-green spaces and impact factors in mega city: A case study of Shanghai (Master's thesis). Retrieved from CNKI database.
- [12] Su, X., Huang, G., Chen, X., & Chen, S. (2010). The cooling effect of Guangzhou City parks to surrounding environments. *Acta Ecologica Sinica*, 30(18), 4905-4918.
- [13] Sun, R., & Chen, L. (2017). Effects of green space dynamics on urban heat islands: Mitigation and diversification. *Ecosystem Services*, (23), 38-46. <https://doi.org/10.1016/j.ecoser.2016.11.011>
- [14] Yu, Z., Guo, X., Zeng, Y., Koga, M., & Vejre, H. (2018). Variations in land surface temperature and cooling efficiency of green space in rapid urbanization: The case of Fuzhou city, China. *Urban forestry and urban greening*, (29), 113-121. <https://doi.org/10.1016/j.ufug.2017.11.008>
- [15] Zhou, D., Zhang, L., Zhang, L., Fan, H., & Liu, D. (2011). The Effect of Landscape Park on Urban Heat Island: A Case Study of Harbin City. *Areal Research and Development*, 30(3), 73-78. doi:10.3969/j.issn.1003-2363.2011.03.015
- [16] Chang, C. -R., Li, M. -H., Chang, S. -D. (2007). A preliminary study on the local cool-island intensity of Taipei city parks. *Landscape and Urban Planning*, 80(4), 386-395. <https://doi.org/10.1016/j.landurbplan.2006.09.005>
- [17] Yu, Z., Xu, S., Zhang, Y., Jørgensen, G., & Vejre, H. (2018). Strong contributions of local background climate to the cooling effect of urban green vegetation. *Scientific Reports*, 8(1), 1-9. Retrieved from <https://www.nature.com/articles/s41598-018-25296-w>
- [18] Fan, H., Yu, Z., Yang, G., Liu, T., Hung, C. H., & Vejre, H. (2019). How to cool hot-humid (Asian) cities with urban trees? An optimal landscape size perspective. *Agricultural and Forest Meteorology*, (265), 338-348. doi:10.1016/j.agrformet.2018.11.027
- [19] Cheng, X., Wei, B., Chen, G., Li, J., & Song, C. (2015). Influence of park size and its surrounding urban landscape patterns on the park cooling effect. *Journal of Urban Planning and Development*, 141(3), A4014002. [https://doi.org/10.1061/\(ASCE\)UP.1943-5444.0000256](https://doi.org/10.1061/(ASCE)UP.1943-5444.0000256)
- [20] Hwang, Y. H., Lum, Q. J. G., & Chan, Y. K. D. (2015). Micro-Scale Thermal Performance of Tropical Urban Parks in Singapore. *Building and Environment*, (94), 467-476. <https://doi.org/10.1016/j.buildenv.2015.10.003>
- [21] Shih, W. (2017). Greenspace patterns and the mitigation of land surface temperature in Taipei metropolis. *Habitat International*, (60), 69-80. <https://doi.org/10.1016/j.habitatint.2016.12.006>
- [22] Monteiro, M. V., Doick, K. J., Handley, P., & Peace, A. (2016). The impact of greenspace size on the extent of local nocturnal air temperature cooling in London. *Urban Forestry and Urban Greening*, (16), 160-169. <https://doi.org/10.1016/j.ufug.2016.02.008>
- [23] Adams, L. M., & Dove, L. E. (1989). Wildlife reserves and corridors in the urban environment: A guide to ecological landscape planning and resource conservation. Columbia: National Institute for Urban Wildlife.
- [24] Jiménez-Muñoz, J. C., Cristóbal, J., Sobrino, J. A., Soria, G., Ninyerola, M., & Pons, X. (2008). Revision of the single-channel algorithm for land surface temperature retrieval from Landsat thermal-infrared data. *IEEE Transactions on Geoscience and Remote Sensing*, 47(1), 339-349. doi:10.1109/TGRS.2008.2007125
- [25] Qin, Z., Karnieli, A., & Berliner, P. (2001). A mono-window algorithm for retrieving land surface temperature from Landsat TM data and its application to the Israel-Egypt border region. *International Journal of Remote Sensing*, 22(18), 3719-3746. <https://doi.org/10.1080/01431160010006971>
- [26] Jiménez-Muñoz, J. C., Sobrino, J. A., Skoković, D., Matter, C., & Cristóbal, J. (2014). Land surface temperature retrieval methods from Landsat-8 thermal infrared sensor data. *IEEE Geoscience and Remote Sensing Letters*, 11(10), 1840-1843. doi:10.1109/LGRS.2014.2312032
- [27] Chandrasekhar, S. (2013). Land surface temperature retrieval methods from Landsat-8 thermal infrared sensor data. *IEEE Geoscience and Remote Sensing Letters*, 11(10), 1840-1843. doi:10.1109/LGRS.2014.2312032
- [28] Yu, Z., Guo, X., Jørgensen, G., & Vejre, H. (2017). How can urban green spaces be planned for climate adaptation in subtropical cities?. *Ecological Indicators*, (82), 152-162. <https://doi.org/10.1016/j.ecolind.2017.07.002>
- [29] Huang, H., Yun, Y., Li, H., Han, S., & Zhu, Y. (2015). Building Density And Hot Island Scale Response Mechanism. *Planners*, 31(12), 101-106. doi:10.3969/j.issn.1006-0022.2015.12.017
- [30] Peng, J., Xie, P., Liu, Y., & Ma, J. (2016). Urban thermal environment dynamics and associated landscape pattern factors: A case study in the Beijing metropolitan region. *Remote Sensing of Environment*, (173), 145-155. <https://doi.org/10.1016/j.rse.2015.11.027>
- [31] Gunawardena, K., Wells, M., & Kershaw, T. (2017). Utilising green and bluespace to mitigate urban heat island intensity. *Science of the Total Environment*, (584), 1040-1055. doi:10.1016/j.scitotenv.2017.01.158
- [32] Jaganmohan, M., Knapp, S., Buchmann, C. M., & Schwarz, N. (2016). The bigger, the better? The influence of urban green space design on cooling effects for residential areas. *Journal of Environmental Quality*, 45(1), 134-145. doi:10.2134/jeq2015.01.0062
- [33] Akbari, H., Kolokotsa, D. (2016). Three decades of urban heat islands and mitigation technologies research. *Energy and Buildings*, (133), 834-842. <https://doi.org/10.1016/j.enbuild.2016.09.067>
- [34] Shi, L., & Zhao, M. (2020). Cool island effect of urban parks and impact factors in summer: A case study of Xi'an. *Journal of Arid Land Resources and Environment*, 34(05), 154-161. doi:10.13448/j.cnki.jalre.2020.139
- [35] Lu, J., Li, C., Yang, Y., Zhang, Y., & Jin, M. (2012). Quantitative evaluation of urban park coolisland factors in mountain city. *Journal of Central South University*, (6), 1657-1662. doi:10.1007/s11771-012-1189-9
- [36] Yu, Z., Guo, H., & Sun, R. (2015). Impacts of urban cooling effect based on landscape scale: A review. *Chinese Journal of Applied Ecology*, 26(2), 636-642.
- [37] Du, H., Song, X., Jiang, H., Kan, Z., Wang, Z., & Cai, Y. (2016). Research on the cooling island effects of water body: A case study of Shanghai, China. *Ecological Indicators*, (67), 31-38. <https://doi.org/10.1016/j.ecolind.2016.02.040>
- [38] Yang, G., Yu, Z., Jørgensen, G., & Vejre, H. (2020). How can urban blue-green space be planned for climate adaption in high-latitude cities? A seasonal perspective. *Sustainable Cities and Society*, (53), 101932. <https://doi.org/10.1016/j.scs.2019.101932>
- [39] Kong, F., Yin, H., James, P., Hutrya, L. R., He, & H. S. (2014). Effects of spatial pattern of greenspace on urban cooling in a large metropolitan area of eastern China. *Landscape and Urban Planning*, (128), 35-47. <https://doi.org/10.1016/j.landurbplan.2014.04.018>
- [40] Akbari, H., & Kolokotsa, D. (2016). Three decades of urban heat islands and mitigation technologies research. *Energy and Buildings*, (133), 834-842. <https://doi.org/10.1016/j.enbuild.2016.09.067>
- [41] McDonald, R., Kroeger, T., Boucher, T., (2016). Planting healthy air: A global analysis of the role of urban trees in addressing particulate matter pollution and extreme heat. Retrieved from [https://thought-leadership-production.s3.amazonaws.com/2016/10/28/17/17/50/0615788b-8eaf-4b4f-a02a8819c68278ef/20160825\\_PHA\\_Report\\_FINAL.pdf](https://thought-leadership-production.s3.amazonaws.com/2016/10/28/17/17/50/0615788b-8eaf-4b4f-a02a8819c68278ef/20160825_PHA_Report_FINAL.pdf)
- [42] Cheng, S., Niu, Y., & Wang, L. (2019). Study on the Mitigation Effect of Parks on the Urban Heat Island Effect—Taking Shenzhen as an Example. *Chinese Landscape Architecture*, 35(10), 40-45. doi:10.19775/j.cla.2019.10.0040